Introduction to Density Functional Theory of Classical Systems: Theory and Applications

Lecturenotes

by
Roland Roth
ITAP, Universität Stuttgart
and
Max-Planck-Institut für Metallforschung, Stuttgart
Germany

Fukuoka, November 2006

Contents

Chapter 1

Introduction

In this lecture I want to cover the basics of density functional theory of classical systems and want to give a flavor of its possible applications.

Density functional theory started as a theory for electrons. Walter Kohn could show that instead of solving the N-particle Schrödinger equation, it is possible to obtain *all* the information of the ground state ($T = 0$) of an electron system from its one-particle density distribution. He went on to show that there exists a functional of the ground state energy that can be written as a functional of the density distribution. This functional possesses two important properties: (i) for the ground state one-particle density distribution this functional recovers the ground state energy of the system, and (ii) for any other one-particle density distribution the functional takes a values that is larger than the ground state energy. Density functional theory was born. About the same time, in the mid 1960s, Mermin showed that these ideas also hold for an electron system at temperature $T > 0$. His formulation of the proof of density function theory was then re-casted for classical systems, i.e. statistical systems that obey the rules of classical mechanics.

While not the first to apply density functional theory to problems of classical statistics, Bob Evans was one who spread the word by his review paper on the gas-liquid interface [4] in which he introduced the formalism of density functional theory to a broad audience. This paper was also my first contact to density functional theory. Closely following Evans' review, we will introduce the formalism of density functional theory in Chapter 2.

Beside the formalism there are the applications of density functional theory. For several systems of great interest there are now reliable and powerful functionals available. Unfortunately, it is in general not possible to construct a density functional from the knowledge of the interparticle interactions alone. In order to construct a functional one needs insight and intuition. One elegant and very successful approach in density functional theory of classical systems is the fundamental measure theory for

hard-sphere mixtures by Yasha Rosenfeld [6]. We will take a close look at this theory in Chapter 3.

Finally, we discuss some typical applications of density functional theory in Chapter 4. These application should demonstrate one of the key points of density functional theory: once a functional for the excess free energy has been found, it is possible to study a large variety of phenomena simply by changing the external potential acting on the system under consideration. We show this for a square-well fluid for which we study the free interface, the fluid at a single planar hard wall, where we observe the drying transition (wetting by the gas phase), and the fluid in a slit geometry, where we observe the capillary evaporation transition.

My hope is it that you as participant of this lecture and reader of this lecture notes get a flavor of what density functional is, how one particular type of functional (the excess free energy functional of the fundamental measure theory) looks like and what it can do. Clearly, it is impossible to cover the whole field of density functional is just a few lectures or on a few pages. The selection of the material reflects my personal experience and taste. After this lecture, however, it should be possible for you to read and understand the literature on density functional theory and its applications.

I would like to thank Prof. Ryo Akiyama for inviting me to give these lectures at the Kyushu University in Fukuoka, Japan, and the *Front Researcher Development Program* of the Kyushu University for their support.

Fukuoka, November 2006 Roland Roth

Chapter 2

Basics of Density Functional Theory

2.1 Short history of DFT

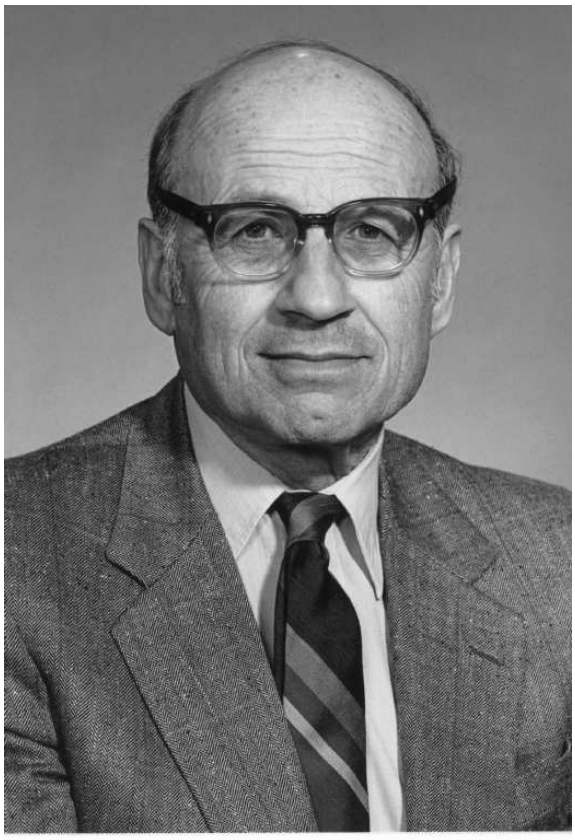

Walter Kohn

- 1964: Hohenberg and Kohn (HK) variational principle for the inhomogeneous electron gas at $T = 0$ (P. Hohenberg and W. Kohn, *Inhomogeneous Electron Gas*, Phys. Rev. **136**, B 864 (1964))

  - electron density $n(\mathbf{r})$ in the ground state $|\Psi\rangle$ as basic variable

$$n(\mathbf{r}) = \langle\Psi|\Phi^*(\mathbf{r})\Phi(\mathbf{r})|\Psi\rangle$$

  - electron density $n(\mathbf{r})$ determines *uniquely* the external potential $V_{ext}(\mathbf{r})$
  - it exists an unique energy functional $E_v[n]$ with the following properties that $E_v[n_0] = E_0$ and $E_v[n \neq n_0] > E_0$.

- 1965: Mermin formulates HK for $T > 0$ (N. D. Mermin, *Thermal Properties of the Inhomogeneous Electron Gas*, Phys. Rev. **137**, A 1441 (1965))
- 1965: Kohn and Sham equations (Kohn and Sham, *Self-Consistent Equations Including Exchange and Correlation Effects*, Phys. Rev. **140**, A 1133 (1965)).
- around 1976: application of DFT to classical systems
- 1998: Nobel Prize in Chemistry for W. Kohn for *his development of the Density Functional Theory*

2.2 Statistical mechanics in the grand canonical ensemble

We start by considering a classical system of N identical particles. The generalization to mixtures is straightforward. Each particle has mass m and is located at position $\mathbf{r}_i$ and has momentum $\mathbf{p}_i$, $i = 1, \ldots N$. The N-particle Hamiltonian is given by

$$H_N = T_{kin} + U + V_{ext},$$

with the kinetic energy

$$T_{kin} = \sum_{i=1}^{N} \frac{p_i^2}{2m},$$

the potential energy of interparticle interaction

$$U = U(\mathbf{r}_1, \ldots, \mathbf{r}_N),$$

and potential energy due to external potential

$$V_{ext} = \sum_{i=1}^{N} V_{ext}(\mathbf{r}_i).$$

Using this Hamiltonian one can calculate the grand canonical partition sum

$$Z_{gc} \equiv Tr_{cl} \exp(-\beta(H_N - \mu N)), \tag{2.1}$$

with $\beta = 1/k_B T$, where k_B is Boltzmann's constant and T the absolute temperature. μ is the chemical potential. Note that in the grand canonical ensemble the system of interest has a volume V, is coupled to a heat bath at temperature T, and to a particle reservoir with chemical potential μ. In Eq. (2.1) we have used the classical trace Tr_{cl} as a shorthand notation for the integral over all particle momenta, all particle positions and the sum over all possible particle numbers $N = 0, \ldots, \infty$. Explicitly, we have

$$Tr_{cl} = \sum_{N=0}^{\infty} \frac{1}{h^{3N} N!} \int d^3 r_1 \ldots \int d^3 r_N \int d^3 p_1 \ldots \int d^3 p_N,$$

where h is Planck's constant.

The grand canonical partition sum Z_{gc} contains *all* the information of the system in thermal equilibrium. From Z_{gc} we can (in principle) calculate everything. If it would be possible to calculate Z_{gc} *exactly*, we would not require the formalism of DFT. However, in general it is not possible to calculate Z_{gc} easily, especially for arbitrary external fields $V_{ext}(\mathbf{r})$. It turns out that it is simpler to make useful approximations within the framework of density functional theory than in the evaluation of the partition sum.

With the help of the partition sum we can define the equilibrium probability density f_0 for N particles at temperature T at particle positions $\mathbf{r}_i$ with momenta $\mathbf{p}_i$, $i = 1, \ldots, N$

$$f_0 \equiv \frac{1}{Z_{gc}} \exp(-\beta(H_N - \mu N)). \tag{2.2}$$

The definition of the probability density is such that the classical trace over the probability distribution gives unity, i.e.

$$Tr_{cl} f_0 = 1$$

Using the equilibrium probability density f_0 we can calculate the (ensemble) averages of operators $\hat{\mathcal{O}}$ by

$$\langle \hat{\mathcal{O}} \rangle \equiv Tr_{cl} f_0 \hat{\mathcal{O}}.$$

One example of such an average, that we will need in the following is the average equilibrium density distribution $\rho_0(\mathbf{r})$ which can be written as the ensemble average over the density operator

$$\rho_0(\mathbf{r}) = \langle \hat{\rho}(\mathbf{r}) \rangle, \tag{2.3}$$

with the density operator

$$\hat{\rho}(\mathbf{r}) = \sum_{i=1}^{N} \delta(\mathbf{r} - \mathbf{r}_i).$$

Finally, we note that the grand potential Ω of the system and the grand canonical partition sum are related via

$$\beta\Omega = -\ln Z_{gc},$$

which is simply the definition of the grand potential.

2.3 Functional of the "grand potential"

Following Mermin [3] we consider the following functional of a probability density f. As mentioned before, we require that the probability density is normalized $Tr_{cl} f = 1$. The functional [3] is given by

$$\Omega[f] = Tr_{cl} f(H_N - \mu N + \beta^{-1} \ln f). \tag{2.4}$$

It possesses the important feature that for the the equilibrium probability density, given by Eq. (2.2) the functional reduces to the grand potential of the system Ω, as can be seen easily from

$$\begin{aligned} \Omega[f_0] &= Tr_{cl} f_0 \left(H_N - \mu N + \beta^{-1} \ln f_0 \right) \\ &= Tr_{cl} f_0 \left(-\beta^{-1} \ln Z_{gc} \right) \\ &= -\beta^{-1} \ln Z_{gc} \\ &\equiv \Omega. \end{aligned}$$

If we now consider a probability distribution different from the equilibrium distribution, i.e. $f \neq f_0$, $Tr_{cl} f = 1$, and we evaluate the functional, Eq. (2.4), we find the inequality

$$\begin{aligned} \Omega[f] &= Tr_{cl} f \left(H_N - \mu N + \beta^{-1} \ln f \right) \\ &= Tr_{cl} f \left(\Omega[f_0] + \beta^{-1} \ln f - \beta^{-1} \ln f_0 \right) \\ &= \Omega[f_0] + \beta^{-1} Tr_{cl} f \left(\ln f - \ln f_0 \right) \\ &> \Omega[f_0], \end{aligned}$$

which is an *important* result, as we shall see in the following. The variational principle of density functional theory is based on this result. In order to show that the inequality holds we used

$$\begin{aligned} H_N - \mu N &= -\beta^{-1} \ln \left(f_0 Z_{gc} \right) \\ &= -\beta^{-1} \ln f_0 - \beta^{-1} \ln Z_{gc} \\ &= -\beta^{-1} \ln f_0 + \Omega[f_0], \end{aligned}$$

which follows directly from the definition of f_0 in Eq. (2.2), and the Gibbs inequality, which we shall discuss in the next Section.

2.4 Gibbs inequality

Here we show that for any two probability densities f_1 and f_2, with $Tr_{cl} f_i = 1$, $i = 1, 2$ we have the inequality

$$Tr_{cl}(f_1 \ln f_1 - f_1 \ln f_2) \geq 0, \tag{2.5}$$

and the equality holds *only* if $f_1 = f_2$. In order to show the inequality we rewrite Eq. (2.5) as

$$\begin{aligned} Tr_{cl}(f_1 \ln f_1 - f_1 \ln f_2) &= Tr_{cl} f_1 (\ln f_1 - \ln f_2) \\ &= Tr_{cl} f_1 \ln \frac{f_1}{f_2} \\ &= Tr_{cl} f_2 \left(\frac{f_1}{f_2} \ln \frac{f_1}{f_2} \right). \end{aligned}$$

Next we observe that there is a *complicated* way of writing a zero by noting that

$$Tr_{cl} f_2 \left(\frac{f_1}{f_2} \right) = Tr_{cl} f_1 = 1,$$

so that we find

$$Tr_{cl} f_2 \left(1 - \frac{f_1}{f_2} \right) \equiv 0$$

Using this observation we can conclude that

$$Tr_{cl} f_2 \left(\frac{f_1}{f_2} \ln \frac{f_1}{f_2} \right) = Tr_{cl} f_2 \left(\frac{f_1}{f_2} \ln \frac{f_1}{f_2} + 1 - \frac{f_1}{f_2} \right) \geq 0. \tag{2.6}$$

In order to see that we obtain this inequality we introduce the variable $x = f_1/f_2$ and rewrite Eq. (2.6) in terms of x as

$$\langle x \ln x - (x - 1) \rangle \geq 0$$

because

$$x \ln x \geq x - 1,$$

as can be seen in Fig. 2.1. Hence we obtain

$$\langle x \ln x \rangle \geq \langle x - 1 \rangle$$

but we have seen before that

$$\langle x - 1 \rangle = 0.$$

It is possible to make the statement of the Gibbs inequality even stronger by noting that $x \ln x = x - 1$ only for $x \equiv f_1/f_2 = 1$. This, however, implies that equality holds

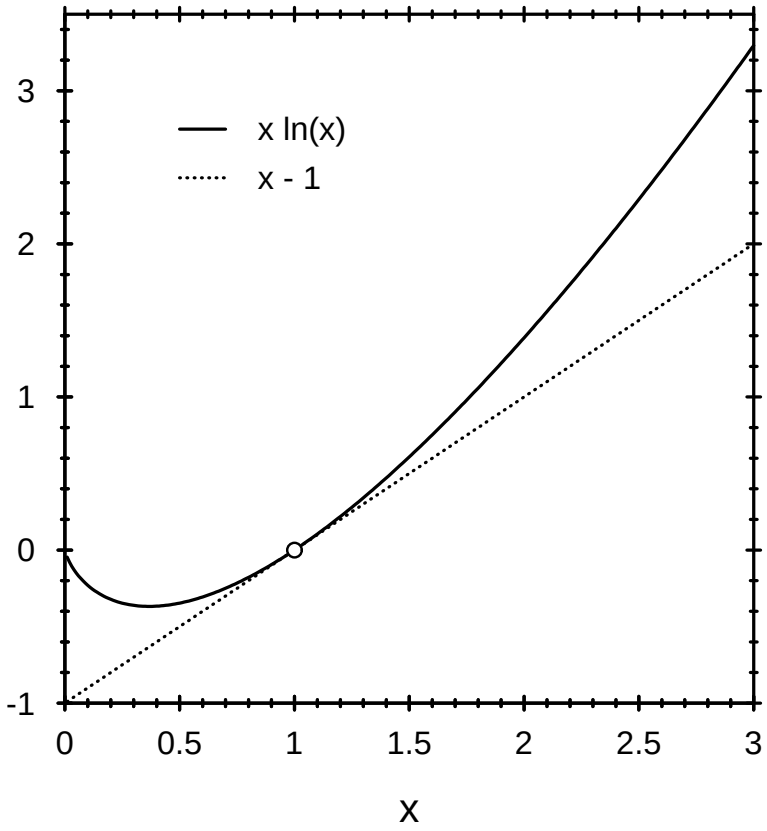

Figure 2.1: $x \ln x$ (full line) is greater or equal $x - 1$ (dotted line), as can be seen in this plot. The equality $x \ln x = x - 1$ holds *only* for $x = 1$, denoted by the circle.

only if $f_1 = f_2$. Thus, if we consider two *different* probability distributions $f_1 \neq f_2$ we can conclude that

$$Tr_{cl}(f_1 \ln f_1 - f_1 \ln f_2) > 0.$$

As a consequence we can deduce that for any a probability distribution different from the equilibrium distribution, i.e. $f \neq f_0$, $Tr_{cl} f = 1$ we obtain the result of the last section

$$\Omega[f] > \Omega[f_0] \equiv \Omega. \tag{2.7}$$

2.5 Hohenberg-Kohn-Mermin variational principle

Through the Hamiltonian H_N, the equilibrium probability distribution f_0, Eq. (2.2), becomes a functional of the external potential $V_{ext}(\mathbf{r})$. It follows that the equilibrium density distribution $\rho_0(\mathbf{r})$ also becomes a functional of $V_{ext}(\mathbf{r})$ though Eq. (2.3). The

next step is to show that f_0 is a functional of $\rho_0(\mathbf{r})$. This can be concluded from the fact that the external potential $V_{ext}(\mathbf{r})$ is uniquely determined by $\rho_0(\mathbf{r})$.

To show this we assume for a moment that a second external field $V_{ext}(\mathbf{r})' \neq V_{ext}(\mathbf{r})$ gives rise to the *same* equilibrium density profile $\rho_0(\mathbf{r})$ (at the same μ and temperature T) and construct a contradiction. The external potentials $V_{ext}(\mathbf{r})$ and $V_{ext}(\mathbf{r})'$ give rise to the Hamiltonians

$$\begin{aligned} H_N &= T_{kin} + U + V_{ext}, \\ H'_N &= T_{kin} + U + V'_{ext}. \end{aligned} \tag{2.8}$$

We also can rewrite H'_N as

$$H'_N = H_N - V_{ext} + V'_{ext}. \tag{2.9}$$

With the help of H_N we can define the equilibrium probability distribution f_0 and with the help H'_N we define $f' \neq f_0$. If we evaluate the functional of the grand potential, Eq. (2.4), for the probability distribution f' we obtain with the help of the Gibbs inequality

$$\begin{aligned} \Omega[f'] &= Tr_{cl} f'(H'_N - \mu N + \beta^{-1} \ln f') \\ &< Tr_{cl} f_0(H'_N - \mu N + \beta^{-1} \ln f_0). \end{aligned}$$

By using Eq. (2.9) the r.h.s. of the inequality can be written first as

$$Tr_{cl} f_0(H'_N - \mu N + \beta^{-1} \ln f_0) = Tr_{cl} f_0(H_N - \mu N + \beta^{-1} \ln f_0 - V_{ext} + V'_{ext})$$

and finally as

$$\Omega[f_0] + Tr_{cl} f_0(V'_{ext} - V_{ext}) = \Omega[f_0] + \int d^3r \rho_0(\mathbf{r}) \left[V'_{ext}(\mathbf{r}) - V_{ext}(\mathbf{r})\right], \tag{2.10}$$

where we have made use of the definition of the equilibrium density distribution, Eq. (2.3). Now we can also evaluate the functional for the distribution f_0:

$$\begin{aligned} \Omega[f_0] &= Tr_{cl} f_0(H_N - \mu N + \beta^{-1} \ln f_0) \\ &< Tr_{cl} f'(H_N - \mu N + \beta^{-1} \ln f') \end{aligned}$$

Again, we follow the same steps as before and rewrite the r.h.s. of the inequality. In addition we make use of our assumption that the distribution f' gives rise to the same equilibrium density distribution $\rho_0(\mathbf{r})$ as f_0. We conclude that the r.h.s. gives

$$\Omega[f'] + Tr_{cl} f'(V_{ext} - V'_{ext}) = \Omega[f'] + \int d^3r \rho_0(\mathbf{r}) \left[V_{ext}(\mathbf{r}) - V'_{ext}(\mathbf{r})\right]. \tag{2.11}$$

By adding Eqs. (2.10) and (2.11) we see that

$$\Omega[f_0] + \Omega[f'] < \Omega[f_0] + \Omega[f']$$

follows, which cannot be true. Therefore the assumption that $V_{ext}(\mathbf{r})$ and $V_{ext}(\mathbf{r})' \neq V_{ext}(\mathbf{r})$ gives rise to the same equilibrium density profile $\rho_0(\mathbf{r})$ is wrong. As a consequence we conclude that the equilibrium probability distribution f_0 is a functional of the equilibrium density distribution $\rho_0(\mathbf{r})$

$$f_0 = f_0[\rho_0(\mathbf{r})],$$

which further implies that the functional of the grand potential, Eq. (2.4), is also a functional of $\rho_0(\mathbf{r})$, i.e.

$$\Omega[f_0] = \Omega[\rho_0].$$

This implies that the functional of the grand potential can be rewritten in the form

$$\Omega[\rho] = \mathcal{F}[\rho] + \int d^3r \rho(\mathbf{r})(V_{ext}(\mathbf{r}) - \mu)$$

with the unique functional of the intrinsic Helmholtz free energy

$$\mathcal{F}[\rho] = Tr_{cl} f(T_{kin} + U + \beta^{-1} \ln f). \tag{2.12}$$

Hence, we can express the functional of the grand potential as a functional of the density distribution $\rho(\mathbf{r})$. This feature is the reason why the theory is called *density functional theory*.

Now we also can rewrite the minimum property of the functional, Eq.(2.7), in terms of density profiles:

$$\Omega[\rho(\mathbf{r}) \neq \rho_0(\mathbf{r})] > \Omega[\rho_0(\mathbf{r})].$$

The main result of this chapter can be summarized by the variational principle

$$\left.\frac{\delta\Omega[\rho]}{\delta\rho(\mathbf{r}))}\right|_{\rho(\mathbf{r})=\rho_0(\mathbf{r})} = 0,$$

which expresses the minimum property in mathematical terms. Furthermore we have for the equilibrium density profile $\rho_0(\mathbf{r})$

$$\Omega[\rho_0] \equiv \Omega.$$

Thus, by *minimizing* the functional of the grand potential we obtain the thermodynamic properties of the system via its grand potential Ω and the structure of the system in form of $\rho_0(\mathbf{r})$.

2.6 Classical analog to Kohn-Sham equations

It is possible to split the intrinsic free energy functional into two parts

$$\mathcal{F}[\rho] = \mathcal{F}_{id}[\rho] + \mathcal{F}_{ex}[\rho],$$

where $\mathcal{F}_{id}[\rho]$ is the intrinsic free energy of an ideal (non interacting) gas. The second contribution, $\mathcal{F}_{ex}[\rho]$, is the excess (over the ideal gas) free energy functional and contains all the information about the interparticle interaction. The ideal gas contribution can be calculated exactly to be

$$\mathcal{F}_{id}[\rho] = \beta^{-1} \int d^3r \rho(\mathbf{r}) \left(\ln \lambda^3 \rho(\mathbf{r}) - 1 \right)$$

with the thermal de Broglie wavelength

$$\lambda = \sqrt{\frac{h^2\beta}{2\pi m}}.$$

Formally, the functional can be minimized through the variational principle. The result is

$$\frac{\delta\Omega[\rho]}{\delta\rho(\mathbf{r})} = 0 = \beta^{-1} \ln \lambda^3 \rho(\mathbf{r}) + \frac{\delta\mathcal{F}_{ex}}{\delta\rho} + V_{ext}(\mathbf{r}) - \mu.$$

We can split the chemical potential $\mu = \mu_{id} + \mu_{ex}$ into an ideal gas contribution $\mu_{id} = \beta^{-1} \ln \lambda^3 \rho_{bulk}$, where ρ_{bulk} is the constant bulk density, and an excess contribution μ_{ex}. The variational principle leads to the self-consistent equations for the density profile

$$\rho(\mathbf{r}) = \rho_{bulk} \exp(-\beta V_{ext}(\mathbf{r}) + c^{(1)}(\mathbf{r}) + \beta\mu_{ex}). \tag{2.13}$$

In this equation we have introduced the one-body direct correlation function

$$c^{(1)}(\mathbf{r}) = -\beta \frac{\delta\mathcal{F}_{ex}[\rho]}{\delta\rho(\mathbf{r})}.$$

Note that for a constant bulk density, the one-body direct correlation function becomes $-\beta\mu_{ex}$. If the external potential is of finite range the argument of the exponential function in Eq. (2.13) vanishes in the limit $\mathbf{r} \to \infty$ when $c^{(1)}(\mathbf{r} \to \infty) \to -\beta\mu_{ex}$. In this limit we obtain $\rho(\mathbf{r} \to \infty) \to \rho_{bulk}$.

This formal solution is not too helpful, because both the left and the right hand side of Eq. (2.13) depend on $\rho(\mathbf{r})$, because $\mathcal{F}_{ex}[\rho]$ and hence $c^{(1)}(\mathbf{r})$ are functionals of the density profile $\rho(\mathbf{r})$. For an ideal gas, for which $\mathcal{F}_{ex}[\rho] = 0$, we can solve for the equilibrium density profile and we find the well-known result

$$\rho_0^{id}(\mathbf{r}) = \rho_{bulk} \exp(-\beta V_{ext}(\mathbf{r})).$$

2.7 Generalization to Mixtures

For completeness we give the form of the functional of the grand potential for a ν component mixture without derivation:

$$\Omega[\{\rho_i\}] = \mathcal{F}_{ex}[\{\rho_i\}] + \sum_{i=1}^{\nu} \beta^{-1} \int d^3r \rho_i(\mathbf{r}) \left(\ln \lambda_i^3 \rho_i(\mathbf{r}) - 1 \right) + \sum_{i=1}^{\nu} \int d^3r \rho_i(\mathbf{r}) \left(V_{ext}^i(\mathbf{r}) - \mu_i \right),$$

with

$$\lambda_i = \sqrt{\frac{h^2\beta}{2\pi m_i}}.$$

The notation $\{\rho_i\}$ indicates that there is a set of density profiles for all components $i = 1, \ldots, \nu$. The excess free energy functional, which is still unspecified, is a functional of *all* density profiles of the mixture. The remaining terms simply turn into sums over all species. In order to minimize the functional of the grand potential one has to solve the coupled equations

$$\left. \frac{\delta\Omega[\{\rho_i\}]}{\delta\rho_i(\mathbf{r})} \right|_{\rho_i(\mathbf{r})=\rho_{0,i}(\mathbf{r})} = 0, \quad i = 1, \ldots, \nu.$$

2.8 Excess free energy $\mathcal{F}_{ex}$

So far we have presented the general formalism of density functional theory. In order to be able to perform any calculation we have to specify the system under consideration, i.e. the interparticle interaction. Formally we then can employ Eq. (2.12) to obtain the functional of the free energy. Unfortunately, this is in practice not possible. This would be equivalent to calculating the partition sum *exactly*.

Since there is no direct way to derive the functional of the excess free energy $\mathcal{F}_{ex}$ from the Hamiltonian, we used as starting point, one requires some approximate schemes to construct the functional. Different approaches prove useful depending on the system under consideration. One system of particular interest is the hard-sphere mixture, which often is used as a reference system for mixtures of simple fluids or for colloidal mixtures. In those cases the short-ranged strong repulsion is mapped onto an hard-sphere diameter and the longer ranged attraction is taken into account through a perturbation theory treatment.

For hard-sphere mixture we have a rather accurate and successful approach called fundamental measure theory (FMT) introduced by Yasha Rosenfeld. We shall discuss this approach in detail in the following chapter.

Chapter 3

Fundamental measure theory

3.1 Introduction

Yasha Rosenfeld

In 1989 Rosenfeld [6] introduced novel ideas for deriving a density functional theory (DFT) for hard-sphere mixtures. His approach, which is distinctly different from earlier non-local, weighted density approximations [5], is based on the fundamental geometrical properties of the spheres and is termed fundamental measure theory (FMT). The original version met with considerable success when applied to a variety of inhomogeneous situations, including the hard-sphere fluid adsorbed at walls and confined in model pores [5, 6]. Although the original version could not describe a stable crystalline phase the FMT was refined [7, 8] in order to incorporate the freezing transition. These refinements and subsequent improvements/modifications of FMT

have all focused on the zero-dimensional ($0D$) limit, i.e. the limit which pertains to a narrow cavity that can contain at most one sphere. Requiring the DFT to yield the exact free energy in the $0D$ limit provided new insight into the structure of FMT and suggested new prescriptions for functionals that could describe situations of extreme confinement [7, 8]. More recently Tarazona and Rosenfeld [9–11] have argued that the hard-sphere free energy functional can be constructed solely from the requirement that the functional reproduces the exact $0D$ limit for cavities of different shapes; the equation of state and the correlation functions of the homogeneous fluid are then given as output from, rather than input to, the DFT. This particular strategy is reviewed briefly in Refs. [10, 12].

One of the main limitations of the original FMT, and indeed of its successors, is that the underlying bulk fluid equation of state is the Percus-Yevick (PY) compressibility equation, equivalent to scaled particle theory. As is well-known, for the case of the pure hard-sphere fluid this implies that the pressure p is overestimated for fluid densities approaching that at bulk freezing [13]. A serious consequence of the inaccuracy of the underlying PY fluid equation of state is that the FMT, suitably modified to include a tensor measure, predicts coexisting fluid and solid densities that are rather low w.r.t. computer simulation results [12].

In this chapter we present a derivation of Rosenfeld's fundamental measure theory functional and then show how the derivation can be adjusted in order to enforce an accurate equation of state, which is done in the White Bear version of FMT [39, 40] and more recently in the White Bear version Mark II [42].

3.2 Exact result in $d = 1$

The structure of Rosenfeld's fundamental measure theory follows the structure of the *exact* excess free energy functional for the ν-component hard-rod mixtures in $d = 1$ [18, 19]. The radius of component i is R_i, so that the length of a rod of component i is $2\ R_i$. A sketch of the system is shown in Fig. 3.1. The derivation of this functional is technical quite involved and is specific to the one-dimensional case. Therefore we shall only quote the functional and its structure, so that we can understand how Rosenfeld got inspired.

The exact excess free energy functional in $d = 1$ can be written as

$$\beta\mathcal{F}_{ex}^{1d}[\{\rho_i\}] = \int dz\ \Phi(\{n_\alpha\}),$$

where Φ is the excess free energy density, which is a *function* (not a functional) of a

set of weighted densities n_α. The weighted densities are defined as

$$n_\alpha(z) = \sum_{i=1}^{\nu} \int dz' \, \rho_i(z') \, \omega_\alpha^i(z - z'),$$

i.e. they are sums over all components $i = 1, \ldots, \nu$ of convolutions of weight functions ω_α^i, which are specific to the geometry of component i. In $d = 1$ one has two different weight functions for each component, namely

$$\omega_0^i(z) = \frac{1}{2} \left(\delta(z - R_i) + \delta(z + R_i) \right),$$

which can be interpreted as a weight function that marks the *surface* of the rod, which consist of the two points at $z - R_i$ and $z + R_i$, and

$$\omega_1^i(z) = \Theta(R_i - |z|),$$

which can be interpreted as a weight function that marks the *volume* of the rod. For the definition of the weight functions we have used the Dirac Delta function $\delta(x)$ and the Heaviside step function $\Theta(x)$, which is 1 for $x > 0$ and 0 otherwise. We can represent the Mayer-f function between a rod of species i and one of species j, which is defined by

$$f_{ij}(z) = \exp(-\beta V_{ij}(z)) - 1 = \begin{cases} -1 & |z| < R_i + R_j \\ 0 & \text{otherwise,} \end{cases}$$

for hard-rod interactions, in terms of weight functions

$$-f_{ij}(z) = \omega_1^i \otimes \omega_0^j + \omega_0^i \otimes \omega_1^j,$$

where the The symbol $\otimes$ denotes the convolution of the weight functions

$$\omega_i^\alpha \otimes \omega_j^\beta(z = z_i - z_j) = \int dz' \, \omega_i^\alpha(z' - z_i) \, \omega_j^\beta(z' - z_j).$$

The excess free energy density is given by

$$\Phi(\{n_\alpha\}) = -n_0 \ln(1 - n_1),$$

which fully specifies the $d = 1$ functional.

It is quite remarkable that the excess free energy possesses such a simple structure.

3.3 Rosenfeld's Fundamental Measure Theory ($d = 3$)

In order to construct a density functional for a mixture consisting of ν species of hard spheres, with $\nu \geq 1$, Rosenfeld used the exact low density result for the excess (over

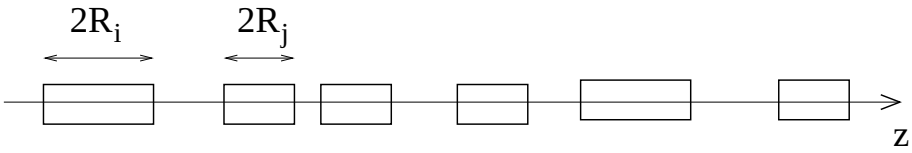

Figure 3.1: Sketch of a one-dimensional hard-rod mixture with radii R_i, $i = 1, \ldots \nu$. The rods can move along a line.

ideal gas) Helmholtz free energy functional, valid in the limit where all the one-body densities $\{\rho_i(\mathbf{r})\} \to 0$,

$$\beta\mathcal{F}_{ex}[\{\rho_i\}] = -\frac{1}{2}\sum_{i,j}\int d^3r \int d^3r' \rho_i(\mathbf{r})\rho_j(\mathbf{r}')f_{ij}(|\mathbf{r}-\mathbf{r}'|) \tag{3.1}$$

as a starting point. He noted that the Mayer-f function between a sphere of component i and one of component j, which is defined, analog to the one-dimensional case, by

$$f_{ij}(r) = \exp(-\beta V_{ij}(r)) - 1.$$

$V_{ij}(r)$ is the pair potential between two species i and j. $f_{ij}(r)$ has a purely geometrical interpretation because of the hard-sphere potential

$$V_{ij}(r) = \begin{cases} \infty & r < R_i + R_j \\ 0 & \text{otherwise}, \end{cases}$$

which gives rise to the Mayer-f function

$$f_{ij}(r) = \begin{cases} -1 & r < R_i + R_j \\ 0 & \text{otherwise}. \end{cases}$$

The Mayer-f function $f_{ij}(r)$ of two hard spheres with radii R_i and R_j marks the volume which is not accessible to the center of one sphere, say of species i, close to the other of species j. This volume is a sphere of radius $R_i + R_j$. In general, the volume of two joined convex bodies V_{i+j} can be written as

$$V_{i+j} = V_i + S_i R_j + R_i S_j + V_j,$$

where V_i, S_i, and R_i are the volume, the surface area and the mean radius of curvature of the body, respectively. The validity of this relation can be checked easily for two spheres where $V_{i+j} = 4\pi/3(R_i + R_j)^3$ and $V_i = 4\pi/3R_i^3$ and $S_i = 4\pi R_i^2$.

Analog to the one-dimensional case, the Mayer-f functions of a hard-sphere mixture can be decomposed into the form

$$-f_{ij}(r) = \omega_3^i \otimes \omega_0^j + \omega_0^i \otimes \omega_3^j + \omega_2^i \otimes \omega_1^j + \omega_1^i \otimes \omega_2^j - \vec{\omega}_2^i \otimes \vec{\omega}_1^j - \vec{\omega}_1^i \otimes \vec{\omega}_2^j \tag{3.2}$$

with the weight functions given by

$$\begin{aligned}
\omega_3^i(\mathbf{r}) &= \Theta(R_i - r), \\
\omega_2^i(\mathbf{r}) &= \delta(R_i - r), \\
\omega_1^i(\mathbf{r}) &= \frac{\omega_2^i(\mathbf{r})}{4\pi R_i} \\
\omega_0^i(\mathbf{r}) &= \frac{\omega_2^i(\mathbf{r})}{4\pi R_i^2} \\
\vec{\omega}_2^i(\mathbf{r}) &= \frac{\mathbf{r}}{r}\delta(R_i - r), \\
\vec{\omega}_1^i(\mathbf{r}) &= \frac{\vec{\omega}_2^i(\mathbf{r})}{4\pi R_i},
\end{aligned}$$

where $\Theta(r)$ is again the Heaviside function and $\delta(r)$ is the Dirac-delta function. The symbol $\otimes$ in Eq. (3.2) denotes the three-dimensional convolution of the weight functions

$$\omega_i^\alpha \otimes \omega_j^\beta(\mathbf{r} = \mathbf{r}_i - \mathbf{r}_j) = \int d\mathbf{r}'\, \omega_i^\alpha(\mathbf{r}' - \mathbf{r}_i)\, \omega_j^\beta(\mathbf{r}' - \mathbf{r}_j).$$

It is important to note that the deconvolution, Eq. (3.2), would appear to be unnecessarily complicated if only a pure hard-sphere fluid were to be considered. For a mixture, however, this particular structure is suggested by that of the *exact* one-dimensional functional of the mixture of hard rods [18, 19] – see Sec. 3.2. It is also interesting to note that an alternative deconvolution of the Mayer-f function, suggested by Kierlik and Rosinberg [20], avoids vector-like weight functions but introduces instead weights containing first and second derivatives of the Dirac-delta function. It was shown later that both deconvolutions are equivalent [21].

The weight functions give rise to a set of weighted densities $\{n_\alpha(\mathbf{r})\}$ for the ν component mixture. These are defined, again analog to the one-dimensional case, as

$$n_\alpha(\mathbf{r}) = \sum_{i=1}^{\nu} \int d^3r' \rho_i(\mathbf{r}')\, \omega_\alpha^i(\mathbf{r} - \mathbf{r}'), \tag{3.3}$$

i.e. the sum of the convolutions of the density profiles of each species with its weight function. α labels the four scalar and two vector weights. In the bulk, where the density profiles in the absence of any external field reduce to constant bulk densities ρ_{bulk}^i, both vector weighted densities $\vec{n}_1$ and $\vec{n}_2$ vanish while the scalar weighted densities reduce to the so-called scaled particle theory (SPT) [24] variables: $n_3 \to \xi_3 = 4\pi \sum_i \rho_{bulk}^i R_i^3/3$, $n_2 \to \xi_2 = 4\pi \sum_i \rho_{bulk}^i R_i^2$, $n_1 \to \xi_1 = \sum_i \rho_{bulk}^i R_i$ and $n_0 \to \xi_0 = \sum_i \rho_{bulk}^i$. Note that ξ_3 then corresponds to the total packing fraction.

As an appropriate ansatz for the excess free-energy functional, Rosenfeld followed again the structure of the exact one-dimensional functional. He wrote the excess free-

energy functional in the form

$$\beta\mathcal{F}_{ex}[\{\rho_i\}] = \int d^3r' \; \Phi(\{n_\alpha(\mathbf{r}')\}) \tag{3.4}$$

where Φ, the reduced free energy density, is a *function* of the weighted densities. As ansatz for Φ Rosenfeld employed dimensional analysis and used

$$\Phi = f_1(n_3)n_0 + f_2(n_3)n_1n_2 + f_3(n_3)\vec{n_1}\cdot\vec{n_2} + f_4(n_3)n_2^3 + f_5(n_3)n_2\vec{n_2}\cdot\vec{n_2}. \tag{3.5}$$

Each term in (3.5) has the dimension of a number density, i.e. [length]$^{-3}$. In order to ensure that the ansatz, Eqs. (3.4) and (3.5), recovers the deconvolution of the Mayer-f function, Eq. (3.2), it is necessary to demand that to lowest order in n_3 the unknown functions f_1, f_2, f_3 have expansions of the form $f_1 = n_3 + \mathcal{O}(n_3^2)$, $f_2 = 1 + \mathcal{O}(n_3^2)$ and $f_3 = -1 + \mathcal{O}(n_3^2)$. $f_4 = 1/24\pi + \mathcal{O}(n_3^2)$, and $f_5 = -3/24\pi + \mathcal{O}(n_3^2)$.

Although the ansatz in Eq. (3.5) is constructed to reproduce *exactly* the low density limit, it is clear that for intermediate and high densities this ansatz introduces the approximation that the weight functions, and hence the weighted densities, required by the low density limit are sufficient to approximate the simultaneous interaction of three or more spheres. This approximation turns into a serious problem in the case of asymmetric mixtures where radii of different components are significantly different [28].

The functions $f_1, \ldots, f_5$ can be determined by demanding that the resulting functional satisfies a thermodynamic condition. In the original derivation Rosenfeld used the SPT equation [24]

$$\lim_{R_i\to\infty} \frac{\mu_{ex}^i}{V_i} = p, \tag{3.6}$$

with $V_i = 4\pi R_i^3/3$, the volume of a spherical particle with radius R_i and μ_{ex}^i the excess chemical potential of species i. This relation relates the excess chemical potential for insertion of a big spherical particle with a radius R_i to the leading order term pV_i, the reversible work necessary to create a cavity big enough to hold this particle. The l.h.s. of Eq. (3.6) can be determined self-consistently in terms of the weighted densities from Eq. (3.5)

$$\beta\mu_{ex}^i = \frac{\partial\Phi}{\partial\rho_i} = \sum_\alpha \frac{\partial\Phi}{\partial n_\alpha}\frac{\partial n_\alpha}{\partial\rho_i}.$$

Due to the geometrical meaning of the weight functions we find $\partial n_3/\partial\rho_i = 4\pi/3R_i^3 \equiv V_i$, $\partial n_2/\partial\rho_i = 4\pi R_i^2 \equiv S_i$, $\partial n_1/\partial\rho_i = R_i$, and $\partial n_0/\partial\rho_i = 1$. In the limit under consideration all but one term vanish and we obtain

$$\lim_{R_i\to\infty} \frac{1}{V_i}\beta\mu_{ex}^i = \frac{\partial\Phi}{\partial n_3}.$$

The equation of state can be obtained from the thermodynamic bulk relation $\Omega_{bulk} = -pV$. Since the grand potential density in the bulk is $\Omega_{bulk}/V = \Phi + f_{id} - \sum_i \rho_{bulk}^i\mu_i$

we obtain

$$\beta p = -\Phi + \sum_\alpha \frac{\partial \Phi}{\partial n_\alpha} n_\alpha + n_0. \tag{3.7}$$

The last term, n_0, results from the ideal gas contribution. We can combine these results in order to obtain the SPT differential equation, Eq. (3.6),

$$\frac{\partial \Phi}{\partial n_3} = -\Phi + \sum_\alpha \frac{\partial \Phi}{\partial n_\alpha} n_\alpha + n_0.$$

By collecting all terms proportional to n_0 one sees that the differential equation for $f_1(n_3)$ takes the form

$$f_1'(n_3)\, n_0(1 - n_3) = n_0,$$

which is solved by

$$f_1(n_3) = const_1 - \ln(1 - n_3),$$

with an integration constant $const_1$ that vanishes. It is easy to find the differential equations for the remaining functions. The integration constants are chosen such that the correct behavior at low densities is recovered. The solution found by Rosenfeld [6] and denoted RF, is

$$\begin{aligned} f_1^{RF}(n_3) &= -\ln(1 - n_3) \\ f_2^{RF}(n_3) &= \frac{1}{1 - n_3} \\ f_3^{RF}(n_3) &= -f_2^{RF}(n_3) \qquad (3.8) \\ f_4^{RF}(n_3) &= \frac{1}{24\pi(1 - n_3)^2} \\ f_5^{RF}(n_3) &= -3 f_4^{RF}(n_3), \qquad (3.9) \end{aligned}$$

and it is straightforward to see that these solutions satisfy the aforementioned conditions for the low density limit. It is worthwhile to note that the conditions $f_3 = -f_2$ and $f_5 = -3f_4$, that fix the dependence of the functional on the vector weighted densities $\vec{n}_1$ and $\vec{n}_2$, follow from Eq. (3.6) only if it is assumed that the SPT differential equation, which is by construction a bulk equation, remains valid for slightly inhomogeneous situations. Since the vector weighted densities vanish in the bulk limit it is, strictly speaking, impossible to determine the functions f_3 and f_5 from bulk thermodynamics alone. Given the success of the Rosenfeld functional in various applications we choose to adopt the conditions (3.8) and (3.9) in the subsequent modifications.

The resulting functional, that we refer to as the original Rosenfeld (RF) functional, is usually written in the form $\Phi = \Phi_1 + \Phi_2 + \Phi_3$ with

$$\Phi_1^{RF} = -n_0 \ln(1 - n_3), \tag{3.10}$$

$$\Phi_2^{RF} = \frac{n_1 n_2 - \vec{n}_1 \cdot \vec{n}_2}{1 - n_3}, \tag{3.11}$$

$$\Phi_3^{RF} = \frac{n_2^3 - 3 n_2 \vec{n}_2 \cdot \vec{n}_2}{24\pi(1 - n_3)^2}. \tag{3.12}$$

Although this functional was found to be very successful and often very accurate in accounting for various properties of highly inhomogeneous fluid phases, it failed to predict the fluid to solid phase transition of the pure hard-sphere system. This failing was first remedied empirically by Rosenfeld *et al.* [7, 8] who modified the dependence of Φ_3 on the weighted densities n_2 and $\vec{n}_2$, taking into account certain features of 'dimensional crossover'. The modifications were found to perform better than the original Rosenfeld DFT for densely packed fluids in spherical cavities – a situation of extreme confinement [25, 26]

Subsequently Tarazona and Rosenfeld derived a FMT especially designed to study the properties of the one-component hard-sphere solid [9–11]. They began with the so-called $0D$-limit which considers a narrow cavity that can hold at most a single sphere. Starting with the free energy function for this narrow pore, functionals are derived for higher embedding dimensions. A three dimensional functional based on this idea reproduces the original Rosenfeld functional. In Ref. [11] it is pointed out, however, that there are shapes of $0D$ cavities which cannot be described by the particular set of weight functions chosen in FMT. The problem becomes more acute with increasing embedding dimension. In three dimensions this prevents the Rosenfeld functional or equivalently a functional based solely on the $0D$ limit from describing the fluid-solid phase transition of the pure hard-sphere system. In order to remedy this defect, Tarazona [11] introduced a new second rank tensor-like weight function $\omega_{m_2}(\mathbf{r})$ and adapted the contribution Φ_3 to the functional. In the notation introduced in Ref. [27], we write the tensor weight function as

$$\omega_{m_2}(\mathbf{r}) = \omega_2(\mathbf{r})(\mathbf{rr}/r^2 - \hat{1}/3), \tag{3.13}$$

with $\hat{1}$ denoting the unit matrix. This gives rise to a new tensor weighted density n_{m_2}. The new Φ_3^T term of the Tarazona FMT is given by [11, 27]

$$\Phi_3^T = \frac{1}{24\pi(1 - n_3)^2} \left(n_2^3 - 3 n_2 \vec{n}_2 \cdot \vec{n}_2 + 9 \left(\vec{n}_2 n_{m_2} \vec{n}_2 - \mathrm{Tr}(n_{m_2}^3)/2 \right) \right), \tag{3.14}$$

and the application of the augmented functional to the hard-sphere solid provided an excellent account of simulation results for the equation of state and for other properties of the solid. The extension of this approach to hard-sphere mixtures requires the introduction of a new third rank tensor-like weight function [28].

3.4 The White Bear Version of FMT

Building upon the ideas presented so far, we are now ready to construct a new functional. We retain the same weight functions and the same form (3.4) for the functional but use a different thermodynamic condition in order to specify the coefficients $f_1, \ldots, f_3$ of the ansatz (3.5). In contrast to existing FMT functionals which output the equation of state [for fluid states this is the Percus-Yevick (PY) compressibility equation] we use the Mansoori-Carnahan-Starling-Leland (MCSL) equation of state [14], which is a generalization to the ν-component hard-sphere fluid of the accurate, one-component Carnahan-Starling equation of state [15], as an *input*. We prescribe the functions $f_1, \ldots, f_5$, retaining the two conditions (3.8) and (3.9), such that the equation of state which underlies the new functional is the MCSL pressure. For this approach to be feasible it is important that the MCSL equation of state is based on the same SPT variables which enter the PY compressibility equation of state underlying the original FMT. The MCSL pressure is given by

$$\beta p_{MCSL} = \frac{n_0}{1-n_3} + \frac{n_1 n_2}{(1-n_3)^2} + \frac{n_2^3}{12\pi(1-n_3)^3} - \frac{n_3 n_2^3}{36\pi(1-n_3)^3}. \tag{3.15}$$

The final term in (3.15) is absent in the PY result.

Incorporating the deconvolution of the Mayer-f function and imposing the conditions (3.8) and (3.9), we employ an ansatz for Φ of the form

$$\Phi = f_1(n_3)n_0 + f_2(n_3)(n_1 n_2 - \vec{n}_1 \cdot \vec{n}_2) + f_4(n_3)(n_2^3 - 3n_2 \vec{n}_2 \cdot \vec{n}_2). \tag{3.16}$$

In order to determine the three unknown functions f_1, f_2, and f_4 we employ Eq. (3.7) in a slightly different way than Rosenfeld did. Instead of the SPT differential equation we demand that thermodynamic pressure, given by Eq. (3.7) equals the MCSL equation of state:

$$-\beta p_{MCSL} = \Phi_{bulk} - \sum_{\alpha=0}^{3} \frac{\partial \Phi_{bulk}}{\partial n_\alpha} n_\alpha - n_0, \tag{3.17}$$

with the sum over the scalar weighted densities only. Substituting (3.15) and (3.16) into (3.17) we obtain differential equations for f_1, f_2 and f_4 by collecting all the terms proportional to n_0, $n_1 n_2$, and n_2^3, respectively. These differential equations can be solved easily and we find $f_1(n_3) = f_1^{RF}(n_3)$, $f_2(n_3) = f_2^{RF}$ and

$$f_4(n_3) = \frac{n_3 + (1-n_3)^2 \ln(1-n_3)}{36\pi n_3^2 (1-n_3)^2} \tag{3.18}$$

The resulting excess free-energy density is given by

$$\Phi = -n_0 \ln(1-n_3) + \frac{n_1 n_2 - \vec{n}_1 \cdot \vec{n}_2}{1-n_3} + (n_2^3 - 3n_2 \vec{n}_2 \cdot \vec{n}_2) \frac{n_3 + (1-n_3)^2 \ln(1-n_3)}{36\pi n_3^2 (1-n_3)^2} \tag{3.19}$$

which should be compared with the original Rosenfeld form, Eqs. (3.10)–(3.12). Note that in the low density limit we obtain $\lim_{n_3\to 0} f_4(n_3) = 1/(24\pi)$, i.e. the same value as from the original Rosenfeld functional [see Eq. (3.12)]. Thus we are guaranteed to recover the exact low density limit.

As the derivation of the new functional has followed that of the original Rosenfeld FMT very closely, it faces similar problems when it is applied to the freezing transition. However, the same procedures that remedied the failings for the original FMT can be used for the new functional. Thus, it is possible to follow the empirical procedure of Refs. [7, 8] and modify the dependence of Φ_3 on the weighted densities n_2 and $\vec{n}_2$ in the new functional. This approach would enable the functional to treat a hard-sphere mixture. Equally well it is possible to follow Tarazona [11] who introduced a tensor-like weighted density in order to study the properties of the *one-component* hard-sphere solid. This is the route we employ here, i.e. in the present calculations for the solid phase we replace the term $(n_2^3 - 3n_2\vec{n}_2\cdot\vec{n}_2)$ in Eq. (3.19) by the numerator of Tarazona's expression (3.14) so that the present Φ_3 is given by

$$\Phi_3 = \frac{n_3 + (1-n_3)^2\ln(1-n_3)}{36\pi n_3^2(1-n_3)^2}\left(n_2^3 - 3n_2\vec{n}_2\cdot\vec{n}_2 + 9\left(\vec{n}_2 n_{m_2}\vec{n}_2 - \mathrm{Tr}(n_{m_2}^3)/2\right)\right). \tag{3.20}$$

3.5 Test for self-consistency

As mentioned earlier, Rosenfeld [6] used the scaled particle equation (3.6) to determine the functions $f_1, \ldots, f_5$. Here we re-examine this equation in the context of self-consistency for the functional.

First we note that the excess chemical potential of inserting a single big hard sphere of species i and radius R_i into a fluid of hard spheres is the reversible work done to create a cavity that is large enough to hold this inserted hard sphere. In SPT one starts with a point-like cavity and increases its size until it is sufficiently large. Clearly, when increasing the cavity size one must work against the pressure of the fluid resulting in a term pV_i, where $V_i = 4\pi R_i^3/3$. Since the surface area of the sphere is also increased, work must also be done against the surface tension. This second term is proportional to the surface area $S_i = 4\pi R_i^2$. Moreover for finite values of R_i the surface tension will also depend on the radius of curvature so there will be an additional term that is proportional to R_i. If, however, we divide the excess chemical potential by the volume V_i it is easy to see that Eq. (3.6) follows and that it is exact in the limit $R_i \to \infty$.

The connection to FMT can be made by noting that the excess chemical potential

takes the form

$$\beta\mu_i^{ex} = \sum_{\alpha=0}^{3} \frac{\partial\Phi_{bulk}}{\partial n_\alpha}\frac{\partial n_\alpha}{\partial\rho_{bulk}^i} \tag{3.21}$$

$$= \frac{\partial\Phi_{bulk}}{\partial n_3}V_i + \frac{\partial\Phi_{bulk}}{\partial n_2}S_i + \frac{\partial\Phi_{bulk}}{\partial n_1}R_i + \frac{\partial\Phi_{bulk}}{\partial n_0}, \tag{3.22}$$

and we used the definition of the SPT variables $n_3, \ldots, n_0$ given earlier. Equation (3.22) has precisely the same form as the SPT expansion so it is clear that for any FMT functional the coefficient of the leading volume term should be identified with βp, i.e. the relation

$$\frac{\partial\Phi_{bulk}}{\partial n_3} = \beta p \tag{3.23}$$

should be obeyed.

In the derivation of the original Rosenfeld functional Eq. (3.23) is *imposed*, i.e. the left hand side of Eq. (3.17) is identified with $-\partial\Phi_{bulk}/\partial n_3$ and the resulting (SPT) differential equation is solved. The pressure which results is the SPT or, equivalently, the Percus-Yevick compressibility equation of state. For the present functional, however, Eq. (3.23) is *not* imposed and we find from Eq. (3.19) that

$$\frac{\partial\Phi_{bulk}}{\partial n_3} = \frac{n_0}{1-n_3} + \frac{n_1 n_2}{(1-n_3)^2} - \frac{n_2^3\left(2+n_3(n_3-5)\right)}{36\pi n_3^2(1-n_3)^3} - \frac{n_2^3\ln(1-n_3)}{18\pi n_3^3}, \tag{3.24}$$

which evidently is different from the MCSL equation of state (3.15). The difference arising from this inconsistency was examined within the context of the one-component fluid where the pressure inputted into the theory is the accurate Carnahan-Starling equation of state, p_{CS}. We show both the Carnahan-Starling equation of state (solid line) and the pressure obtained from Eq. (3.24) (dashed line) in Fig. 3.2. The deviation between these two curves is at most 2%. In contrast, the Percus-Yevick compressibility equation of state p_{PY}^c, also shown in Fig. 3.2 (dotted line), overestimates the pressure of a hard-sphere fluid close to freezing by up to 7%.

3.6 The White Bear Version of FMT Mark II

Based on the observation that the MCSL equation of state leads to a excess free energy density that is slightly inconsistent, recently a new generalization of the Carnahan-Starling equation of state to mixtures was proposed [41]

$$\beta p_{\rm CSIII} = \frac{n_0}{1-n_3} + \frac{n_1 n_2\left(1+\frac{1}{3}n_3^2\right)}{(1-n_3)^2} + \frac{n_2^3\left(1-\frac{2}{3}n_3+\frac{1}{3}n_3^2\right)}{12\pi(1-n_3)^3}\,.$$

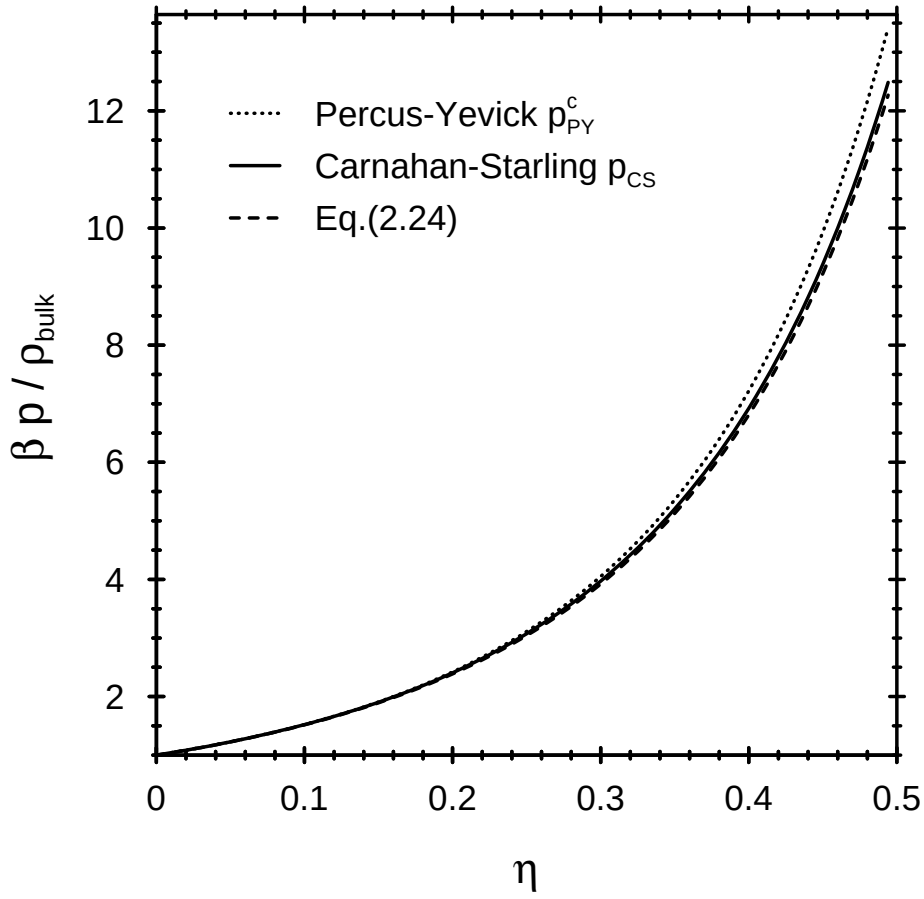

Figure 3.2: The equation of state of the pure hard-sphere fluid versus packing fraction $\eta = \rho_{bulk} 4\pi/3R^3$. For the present DFT the Carnahan-Starling pressure is imposed by the theory. The pressure given by $\partial\Phi_{bulk}/\partial n_3$ in Eq. (3.24) deviates very slightly from Carnahan-Starling, attesting to the high degree of self-consistency of the approach.

This equation of state reduces to the Carnahan-Starling equation of state in the one-component case and represents data for binary and ternary mixtures obtained by computer simulations more accurate than the MCSL result. Based on this new equation of state we can, following the derivation of Sec. 3.4, derive an excess free energy functional, which improves the level of self consistency. We find [42]

$$\begin{aligned}\Phi_{\mathrm{WBII}} &= -n_0\ln(1-n_3) + \left(1+\tfrac{1}{9}n_3^2\phi_2(n_3)\right)\frac{n_1n_2-\vec{n}_1\cdot\vec{n}_2}{1-n_3} \\ &\quad + \left(1-\tfrac{4}{9}n_3\phi_3(n_3)\right)\frac{n_2^3-3n_2\vec{n}_2\cdot\vec{n}_2}{24\pi(1-n_3)^2} \end{aligned} \tag{3.25}$$

with

$$\phi_2(n_3) = \left(6n_3 - 3n_3^2 + 6(1-n_3)\ln(1-n_3)\right)/n_3^3,$$

and

$$\phi_3(n_3) = \left(6n_3 - 9n_3^2 + 6n_3^3 + 6(1-n_3)^2\ln(1-n_3)\right)/(4n_3^3).$$

This functional is similar in complexity as the White Bear version, Eq. 3.19, or the Rosenfeld functional, but is constructed such that for a one-component fluid we find

$$\frac{\partial\Phi_{bulk}}{\partial n_3} = \beta p_{CS},$$

with Carnahan-Starling equation of state p_{CS}.

Chapter 4

Application

4.1 Introduction

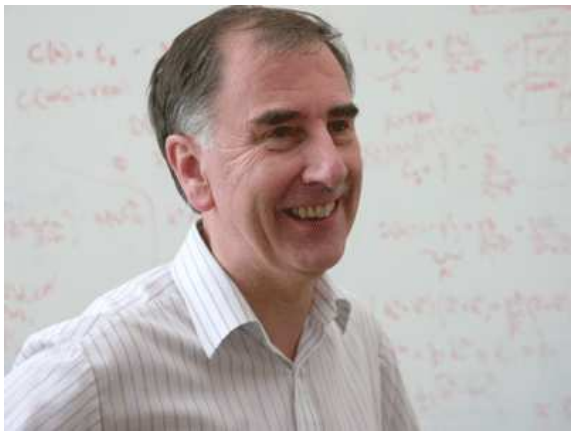

Bob Evans

Bob Evans wrote the first review on density functional theory for classical systems in 1979 [4], just a few years after the theory was *translated* from quantum mechanical systems to classical ones. He was among the first to realize the power of density functional theory and pioneered several of its application. With his review article [4] Bob Evans inspired and influenced many people and made density functional theory for classical system available to a broad audience. My first contact to density functional theory was by reading his papers on the subject.

4.2 Hard-Sphere Fluid at a Hard Wall

The first example application we discuss here is one of the simplest inhomogeneous system one can consider: a hard-sphere fluid at a planar hard wall. Note that in the case of a fluid the equilibrium density profile $\rho_0(\mathbf{r})$ has the same symmetry as the external

potential. For the planar hard wall this means that $\rho_0(\mathbf{r}) = \rho_0(z)$. All interactions are hard-core like which makes temperature a simple scaling parameter. The only parameter in the system is the bulk density ρ_{bulk} or equivalently the bulk packing fraction $\eta = \rho_{bulk}\frac{4\pi}{3}R^3$, where R is the radius of the spheres.

The general outline of the problem of finding the equilibrium density profile $\rho_0(z)$ is as follows:

- choose liquid density ρ_{bulk} or packing fraction $\eta = \rho_{bulk}\frac{4\pi}{3}R^3$
- initialize density profile

  $$\rho(z) = \rho_{bulk}\exp(-\beta V_{ext}(z))$$

  with

  $$\beta V_{ext}(z) = \begin{cases} \infty & z < R \\ 0 & \text{otherwise} \end{cases}$$

- minimize the density functional

  $$\frac{\delta\Omega[\rho]}{\delta\rho(\mathbf{r})} = 0$$

There are several points to be addressed in order to make clear what we mean by *minimizing the density functional* and how we perform this task in practice. Functional minimization is a standard problem in numerical mathematics and there are several more or less clever algorithms available. Each algorithm has its advantages as well as drawbacks. In the present context we wish to keep things as simple as possible and restrict our consideration to a simple Picard iteration, which is in general robust but converges slower than a clever minimization.

4.2.1 Minimizing $\Omega[\rho]$ through a Picard Iteration

First I give the four simple steps of the Picard iteration and then I discuss their meaning.

1. initialize density profile: $\rho^{(0)}(z) = \rho_{bulk}\exp(-\beta V_{ext}(z))$
2. calculate [see Eq. (2.13)] using $\rho^{(i)}(z)$

   $$\tilde{\rho}^{(i)}(z) = \rho_{bulk}\exp(-\beta V_{ext}(z) + c^{(1)}(z) + \beta\mu_{ex})$$

3. mix solutions with mixing parameter α

   $$\rho^{(i+1)}(z) = (1-\alpha)\rho^{(i)}(z) + \alpha\tilde{\rho}^{(i)}(z)$$

4. goto step 2 until solution is converged

The initialization given here is only one possible choice. The closer this initial guess is to the equilibrium density distribution the faster the minimization will converge. Often, however, it is very difficult to have a good guess. If the external field is strongly attractive, then the choice given here can turn out to be a bad one. Once an initial profile is chosen we can start with the iteration. In step 2 we use Eq. (2.13) to calculate a different guess, which we call $\tilde{\rho}^{(i)}(z)$. Clearly, if we input the equilibrium density profile into the r.h.s. of Eq. (2.13), we again recover the equilibrium density profile from the l.h.s. of Eq. (2.13). If we input any other density profile we obtain a different guess for the density profile. In order to keep the iteration from making too rapid changes, which might result in unphysical density distributions such as negative densities or local packing fraction larger than 1, it is useful to mix the old and the new guess, as specified in step 3. The choice of the mixing parameter α is very important. If we choose it too small, the convergence of the iteration is very slow. If we choose it too large, we end up with the same problem mentioned above: the changes in the density profile might be too rapid and one might end up with an unphysical result. Step 4 is to check if the iteration converged already. If the change in the density profile is smaller than a threshold then we can stop the iteration.

In the course of the minimization either through the described iteration or through any other algorithm one has to calculate the weighted densities $n_\alpha(z)$ from a given density distribution very often.

4.2.2 Weighted Densities

Here, to keep our considerations simple, we restrict ourself to a planar geometry. For any (not just hard-wall) external potential that possesses a planar geometry so that $V_{ext}(\mathbf{r}) = V_{ext}(z)$, where z is the distance normal to the wall, a ***fluid*** density profile also possesses the planar geometry: $\rho(\mathbf{r}) = \rho(z)$. It is easy to show that the weighted densities, Eq. (3.3), also take on the planar geometry, i.e. $n_\alpha(\mathbf{r}) = n_\alpha(z)$. By using the symmetry of the problem, one can perform two of the three integrals in Eq. (3.3) analytically and thereby reduce the calculation of the weighted densities to a single integral. In the planar geometry one finds that this integral is of the convolution type, just as the original three-dimensional integral in Eq. (3.3). Note it is not always the case that a three-dimensional convolution integral remains a convolution after some integrals are performed analytically. For example, in the cylindrical geometry, one looses the convolution property by performing two integrals analytically, in the spherical geometry, however, one finds results similar to the planar geometry.

One finds that

$$n_\alpha(\mathbf{r}) = n_\alpha(z) = \int dz'\, \rho(z')\, \omega_\alpha(z - z')$$

with the *one-dimensional* weight functions $\omega_3(z) = \pi(R^2 - z^2)$, $\omega_2(z) = 2\pi R$, and $\vec{\omega}_2(z) = 2\pi z \vec{e}_z$, with the unity vector in the direction normal to the wall $\vec{e}_z$. The remaining weight functions are related to $\omega_2(z)$ and $\vec{\omega}_2(z)$ via $\omega_1(z) = \omega_2(z)/(4\pi R)$, $\omega_0(z) = \omega_2(z)/(4\pi R^2)$, and $\vec{\omega}_1(z) = \vec{\omega}_2(z)/(4\pi R)$.

Since the integrals are still convolutions one can exploit the convolution theorem and perform the calculation in Fourier space, where the convolution is a simple multiplication. Using the FFT (fast Fourier transform) we get

$$\int dz'\, \rho(z')\, \omega_\alpha(z - z') = \mathcal{FT}^{-1}\left(\mathcal{FT}(\rho) * \mathcal{FT}(\omega_\alpha)\right),$$

where $\mathcal{FT}$ denotes the fast Fourier transform of a function and $\mathcal{FT}^{-1}$ the fast inverse Fourier transform. The advantage of using FFT is the speed. Convolutions performed in Fourier space are in general much faster than those performed in real space. If one wants to implement an integration scheme of higher order, which is straightforward in the real space, one has to be careful in Fourier space.

Once the weighted densities are evaluated, one is ready to calculate the one-body direct correlation function $c^{(1)}(z)$

4.2.3 One-Body Direct Correlation $c^{(1)}(z)$

From the definition of the one-body direct correlation function and the structure of the excess free energy functional within fundamental measure theory one finds

$$c^{(1)}(z) = -\beta \frac{\delta \mathcal{F}_{ex}[\rho]}{\delta \rho(z)} = -\int dz' \sum_\alpha \frac{\partial \Phi(\{n_{\tilde{\alpha}}\})}{\partial n_\alpha} \frac{\delta n_\alpha(z')}{\delta \rho(z)}.$$

The main problem is to calculate the variation of the weighted densities $n_\alpha(z')$ w.r.t. the density profile $\rho(z)$. The result (in planar geometry) is quite simple

$$\frac{\delta n_\alpha(z')}{\delta \rho(z)} = \frac{\delta}{\delta \rho(z)} \int dz''\, \rho(z'')\, \omega_\alpha(z' - z'') = \omega_\alpha(z' - z).$$

However, one has to be careful because of the argument of the weight function. Compared to the argument entering the weight function of the weighted densities, the argument entering the calculation of $c^{(1)}(z)$ is negative, i.e. $z - z'$ becomes $z' - z$. For the scalar weight functions this is unimportant, since the scalar weight functions are even

$$\omega_\alpha(z' - z) = \omega_\alpha(z - z'),$$

but the vector-like weight functions are odd

$$\vec{\omega}_\alpha(z' - z) = -\vec{\omega}_\alpha(z - z').$$

Taking this sign into account, it is possible to perform the convolutions in Fourier space using FFT methods:

$$c^{(1)}(z) = -\sum_\alpha \mathcal{FT}^{-1}\left(\mathcal{FT}(\frac{\partial\Phi(\{n_{\tilde{\alpha}}\})}{\partial n_\alpha}) * \mathcal{FT}(\pm\omega_\alpha)\right).$$

4.2.4 Hard-Sphere Fluid at a Hard Wall: the density profile

After discussing the practical issues of minimizing a fundamental measure theory density functional, we can have a look at a typical density profile of a hard-sphere fluid at a planar hard wall. The packing fraction is choose to be $\eta = \rho_{bulk}\frac{4\pi}{3}R^3 = 0.4257$, which is quite high. Note that for $\eta > 0.494$ hard spheres freeze and form a fcc crystal.

In Fig. 4.1 we show the result. The full line denotes the density profile of the White Bear version of FMT, the dashed line that of the original Rosenfeld functional and the symbols denote results obtained from simulation [30]. The results from the two version of DFT lie almost on top of each other except for values of z very close to contact (see inset). The reason for the small deviation close to the wall is the contact theorem, which states that at a planar hard wall the contact density $\rho(R^+)$ is equal to the bulk pressure

$$\rho(R^+) = \beta p,$$

where R^+ indicates that the contact value of the density profile is the value at $z = R$ plus an infinite displacement.

The equation of state underlying the Rosenfeld functional is the Percus-Yevick compressibility pressure, which is known to overestimate the actual pressure of the hard-sphere fluid. By construction, the equation of state of the White Bear version of FMT is the Carnahan-Starling pressure, which is closer to the pressure of the hard-sphere fluid and agrees well with computer simulations.

There are several other properties of the one-component hard-sphere system in the fluid and the crystal phase studied in detail [39]. In general the agreement found with simulations is excellent. Hard-sphere mixtures can also be studied within FMT [34]. If the size ratio is not too asymmetric the agreement with simulations is very good. As the sizes of the species in the mixture get more asymmetric some problems of FMT functionals become apparent [28].

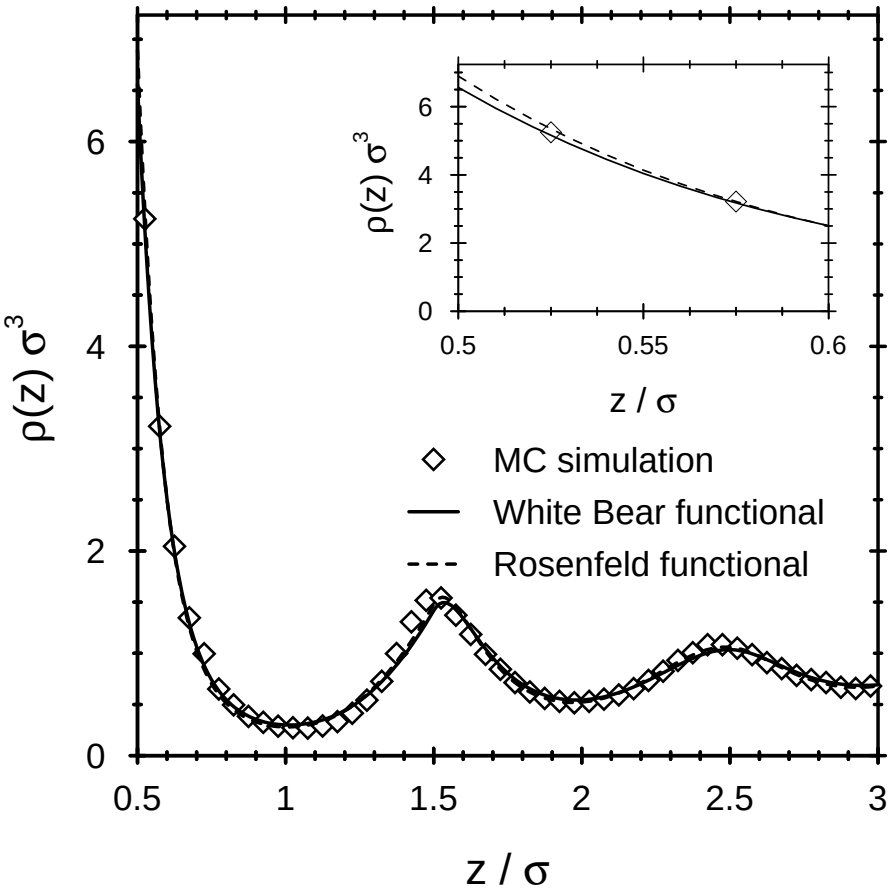

Figure 4.1: Density profile of a one-component hard-sphere fluid at a planar hard wall for $\eta = 0.4257$.

4.3 Square-Well Fluid

The hard-sphere fluid is often employed as a useful reference system for a fluid with a hard-core repulsion at short separation and an additional attraction. As an example for such a fluid we consider a fluid with a square-well interparticle interaction given by

$$\beta V_{sw}(r) = \begin{cases} \infty & r < 2R \\ -\varepsilon & 2R < r < 2R_{sw} \\ 0 & \text{otherwise.} \end{cases}$$

R_{sw} denotes the square-well radius. Even for such a simple interparticle interaction potential it is in general not possible to construct a density functional of the intrinsic excess free energy $\mathcal{F}_{ex}$ analog to the fundamental measure theory for hard-sphere mixtures. Very often the additional attraction is taken into account in an perturbative way

by splitting the excess free energy into a hard-sphere contribution plus a perturbation

$$\mathcal{F}_{ex}[\rho] = \mathcal{F}_{ex}^{HS}[\rho] + \frac{1}{2}\int d^3r\rho(\mathbf{r})\int d^3r'\rho(\mathbf{r}')\,\phi_{sw}(|\mathbf{r}-\mathbf{r}'|).$$

The perturbation term underestimates the correlation in the system. To compensate this effect, one usually introduces a modified square-well potential

$$\beta\phi_{sw}(r) = \begin{cases} -\varepsilon & r < 2R_{sw} \\ 0 & \text{otherwise}, \end{cases}$$

where the square-well is extended into the core, i.e. to $r \to 0$. While this seems physical meaningless at first, it helps to *empirically* correct for the error in the correlations.

4.3.1 Bulk Fluid Phase Diagram

In the following we will restrict the considerations to the fluid phase and neglect the possibility of crystallization. In the fluid phase, if the temperature is sufficiently small, the square-well fluid can phase separate into a low density gas and a high density liquid. In order to locate at which temperatures this phase separation can take place we require the chemical potential and the equation of state, which can be obtained from the density functional, by inputting a constant density profile $\rho(\mathbf{r}) = \rho_{bulk}$. The resulting chemical potential is

$$\mu(\rho_{bulk}) = \left.\frac{\partial f}{\partial\rho}\right|_{\rho=\rho_{bulk}} = \mu_{HS}(\rho_{bulk}) - \varepsilon\eta\left(\frac{R_{sw}}{R}\right)^3 + \ln\lambda^3\rho_{bulk},$$

with a hard-sphere contribution $\mu_{HS}(\rho_{bulk})$, a square-well contribution, and an ideal gas term $\ln(\lambda^3\rho_{bulk})$. At first it seems as if the value of λ and hence of the mass of the particles plays an role in determining the phase diagram. However, this is not the case and one can see easily that the value of λ shift the value of μ but does not affect the phase diagram at all. Therefore, it is possible to replace the ideal gas contribution to the chemical potential, $\ln\lambda^3\rho_{bulk}$ by a simpler term of the form $\ln\eta$, which is equivalent to a particular choice of λ.

The equation of state follows from the grand potential of a bulk system to be

$$p(\rho_{bulk}) = \mu(\rho_{bulk})\rho_{bulk} - f(\rho_{bulk}) = p_{HS}(\rho_{bulk}) - \frac{\varepsilon}{2}\rho_{bulk}\eta\left(\frac{R_{sw}}{R}\right)^3,$$

with the hard-sphere equation of state of the reference system and a square-well term. In order to describe a phase equilibrium between two fluid phases I and II with corresponding densities ρ_I and ρ_{II}, we demand chemical and mechanical equilibrium

$$\mu(\rho_I) = \mu(\rho_{II}) \quad \text{and} \quad p(\rho_I) = p(\rho_{II}).$$

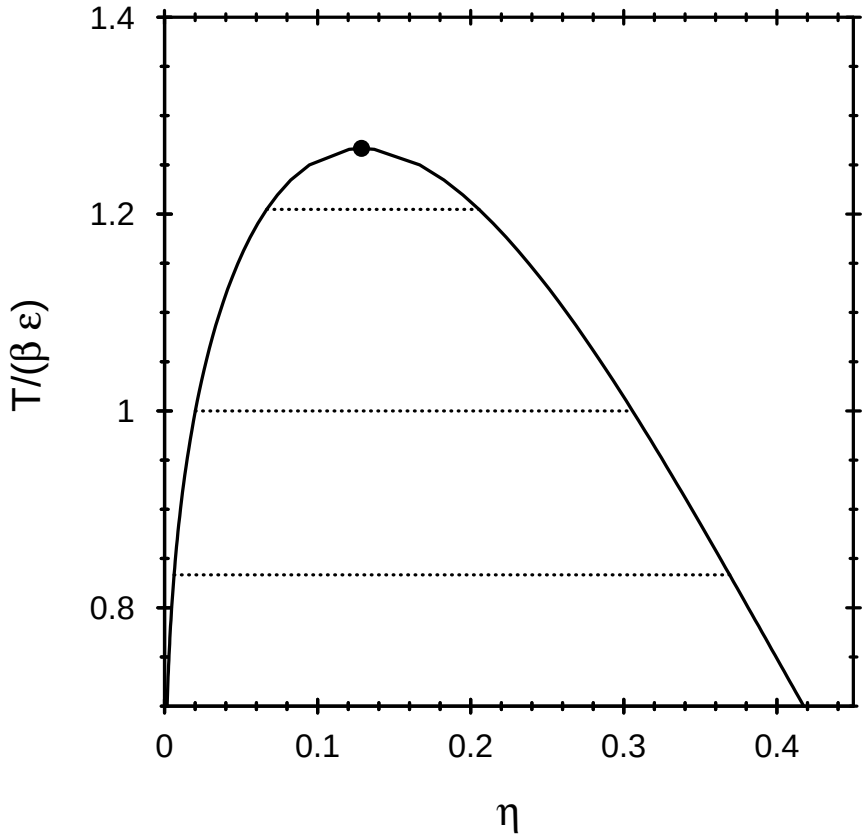

Figure 4.2: The bulk fluid phase diagram of a square-well fluid with $R_{sw} = 3R$. The full circle denotes the critical point. Below the critical temperature the fluid can phase separate into a low density gas and a high density liquid.

Note that these conditions can be fulfilled only at sufficiently low temperatures, where the equation of state and the chemical potential display van der Waals loops. The temperature at which these loops appear is called the critical temperature T_c. To locate the critical temperature one demands that the first and the second derivative of the pressure w.r.t. the density vanishes, i.e.

$$\left.\frac{\partial p}{\partial \rho}\right|_{T=T_c} = 0 \quad \text{and} \quad \left.\frac{\partial^2 p}{\partial \rho^2}\right|_{T=T_c} = 0.$$

For $T < T_c$, the system can separate into a low density gas and a high density liquid phase.

The bulk fluid phase diagram for a square-well radius of $R_{sw} = 3R$ is shown in Fig. 4.2 in the η-T representation. The critical point is denoted by the full circle. Below the critical temperature a low density gas and a high density liquid can coexist, if their respective densities are on the binodal (full line). The coexistence is indicated for the

temperatures $T/(\beta\varepsilon) = 1.2$, 1.0 and 0.83 by the dotted lines. Outside the binodal line there are single phase regions. At densities below the coexisting gas density, the gas phase is the single stable bulk phase and at densities above the coexisting liquid density, the liquid phase is the single stable bulk phase. Inside the binodal line there is a region of metastable and unstable states, which shall not be discussed here.

4.3.2 Free Interface

In the case of bulk coexistence between a low density gas and a high density liquid one finds an inhomogeneous density distribution of the free interface. The interface is called free, because it can form without the presence of an external field, i.e. in the bulk.

The calculation of the free interface density profile can be done by the following steps:

- for a fixed temperature $T < T_c$ choose coexisting densities ρ_I and ρ_{II} so that

$$\mu(\rho_I) = \mu(\rho_{II}) \quad \text{and} \quad p(\rho_I) = p(\rho_{II})$$

- initialize density profile

$$\rho(z) = \begin{cases} \rho_I & z < 0 \\ \rho_{II} & z > 0 \end{cases}$$

- minimize density functional

$$\frac{\delta\Omega[\rho]}{\delta\rho(\mathbf{r})} = 0$$

Note that the minimization has to be performed while enforcing the boundary conditions: for $z \ll 0$ the density profile approaches ρ_I and for $z \gg 0$ it approaches ρ_{II}.

For the temperatures $T/(\beta\varepsilon) = 1.2$, 1.0 and 0.83, marked by the dotted lines in Fig. 4.2, we show the density profiles of the free interface in Fig. 4.3.

For the lowest temperature considered, $T/(\beta\varepsilon) = 0.83$, the difference in the coexisting densities is considerably large, as can be seen in the phase diagram shown in Fig. 4.2. The width of the corresponding interface, the region where the density goes from the a gas-like density to a liquid-like density, is of the order of $4R$. Note that on the liquid side of the interface one can see the onset of an oscillatory structure.

As we increase the temperature to $T/(\beta\varepsilon) = 1.0$ and 1.2, the difference in the coexisting densities becomes smaller and the interface broader, which is to be expected

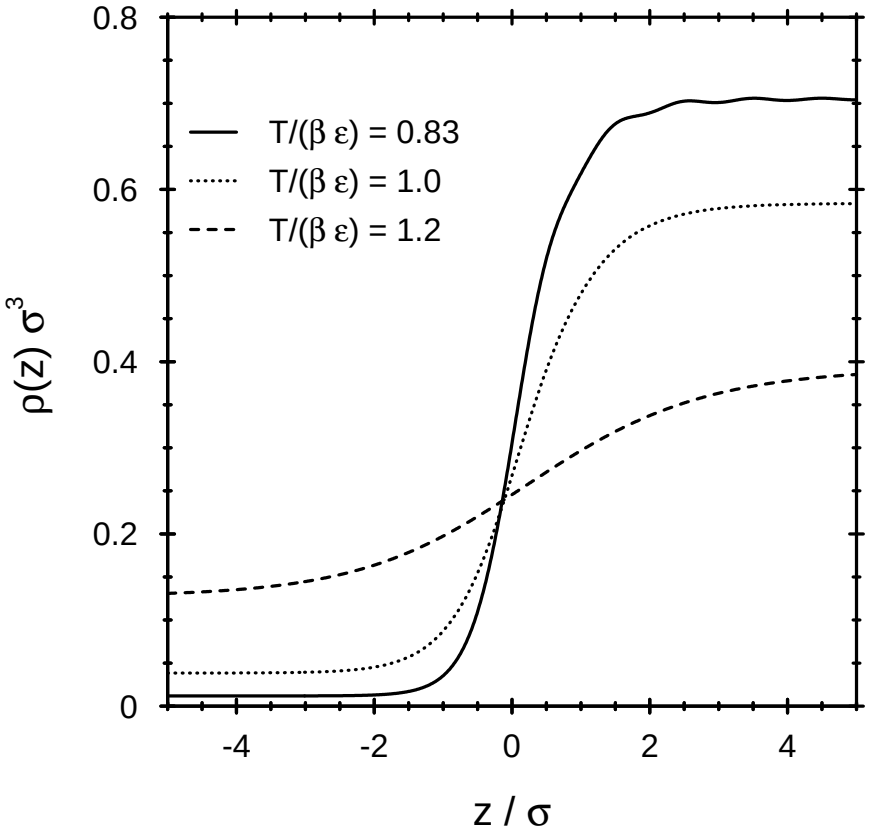

Figure 4.3: The free interface of a square-well fluid at three different temperatures – see Fig. 4.2. $\sigma = 2R$ is the hard-sphere diameter.

as we approach the critical point. At the critical point, the difference between the gas and the liquid density vanishes and so does the interface.

The free interface density profiles predicted by density functional theory are smooth functions which do not display the fluctuations caused by the capillary waves.

4.3.3 Surface Tension of the Free Interface

From the density profiles $\rho_0(z)$ of the free interface we can calculate the energy cost of the formation of the interface. The grand potential of the system is given by

$$\Omega = \Omega[\rho_0(z)].$$

The energy cost is measured by the liquid (l) and vapor (v) interface tension γ_{lv}, which is defined by

$$\gamma_{lv} = \frac{1}{A}\left(\Omega - \Omega_{bulk}\right) = \frac{1}{A}\left(\Omega[\rho_0(z)] + pV\right),$$

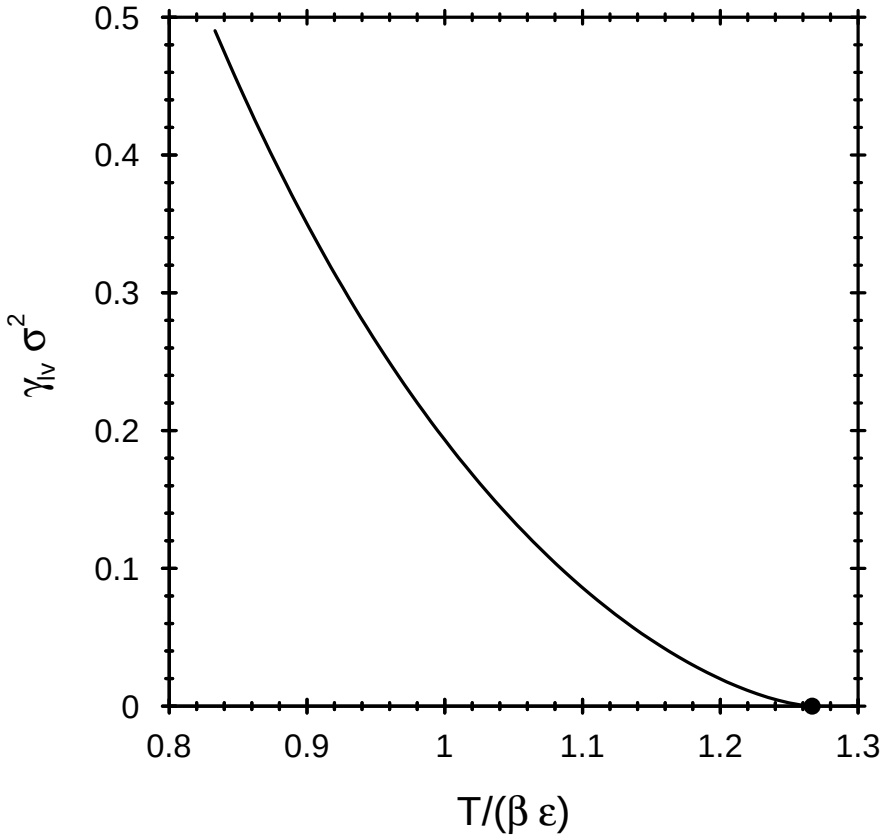

Figure 4.4: The interfacial tension γ_{lv} of a square-well fluid as a function of temperature. $\sigma = 2R$ is the hard-sphere diameter.

with the area of the interface A and $\Omega_{bulk} = -pV$. As the critical point is approached (from below, i.e. $T < T_c$), the energy cost of the interface formation becomes smaller and at the critical point, at which the interface vanishes, the liquid-vapor interfacial tension γ_{lv} vanishes.

The result for the interfacial tension γ_{lv} is shown in Fig. 4.4. Close to the critical point, indicated by the full circle, the interfacial tension γ_{lv} vanishes with a power law, according to the theory of critical phenomena. However, the exponent of the power law is predicted by density functional theory is the (incorrect) mean-field exponent. To determine the correct power law is quite involved and shall not be discussed here.

4.3.4 Square-Well Fluid at a Hard Wall

The next problem we consider is the inhomogeneous density distribution of a square-well fluid close to a planar hard-wall. For a particular interesting behavior, we restrict our considerations here to temperatures T below the critical temperature, i.e. $T < T_c$,

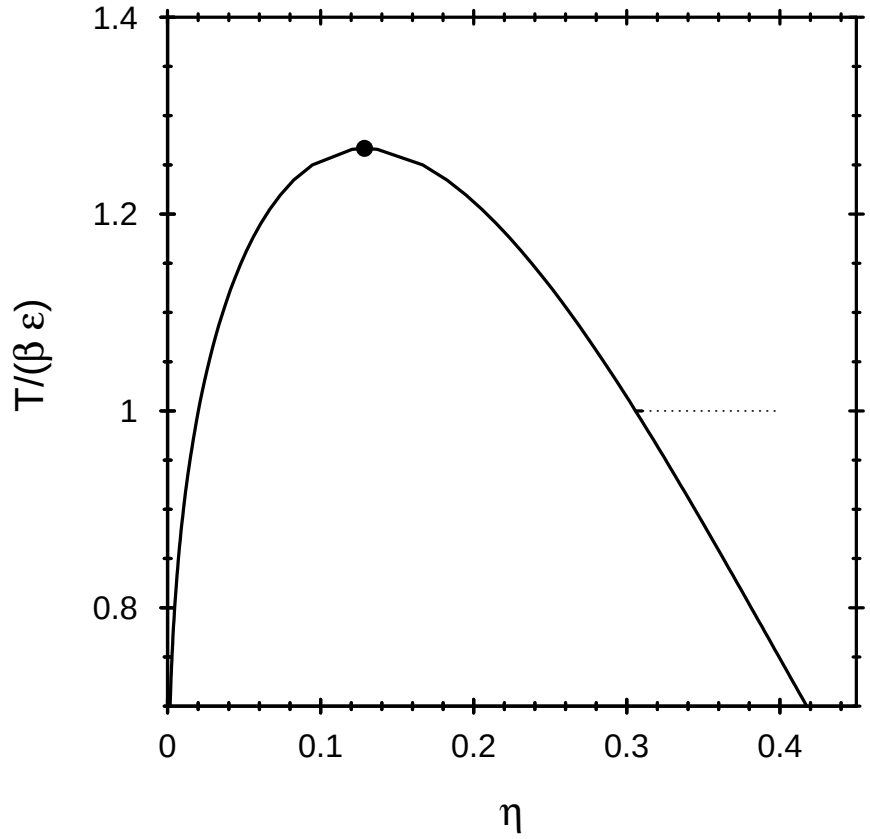

Figure 4.5: The path through the phase diagram is indicated by the full line. The dashed line is a guide to the eye.

and to liquid densities ρ_{bulk}, away from the binodal line. The path we take in the phase diagram is shown in Fig. 4.5. We fix the temperature at $T/(\beta\varepsilon) = 1.0$ and consider the liquid packing fractions η=0.31000, 0.30610, and 0.30571. The coexisting liquid density at this temperature is at $\eta_{co} = 0.305700789$. The actual path is indicated by the full line in Fig. 4.5 at the temperature $T/(\beta\varepsilon) = 1.0$. Since all values of η considered here are rather close to the coexisting density, we also plot, as a guide to the eye, the dashed line.

The density profile of the square-well fluid close to a planar hard wall can be calculated by the following steps:

- choose liquid density ρ_{bulk} or packing fraction η, $T < T_c$
- initialize density profile

$$\rho(z) = \rho_{bulk} \exp(-\beta V_{ext}(z))$$

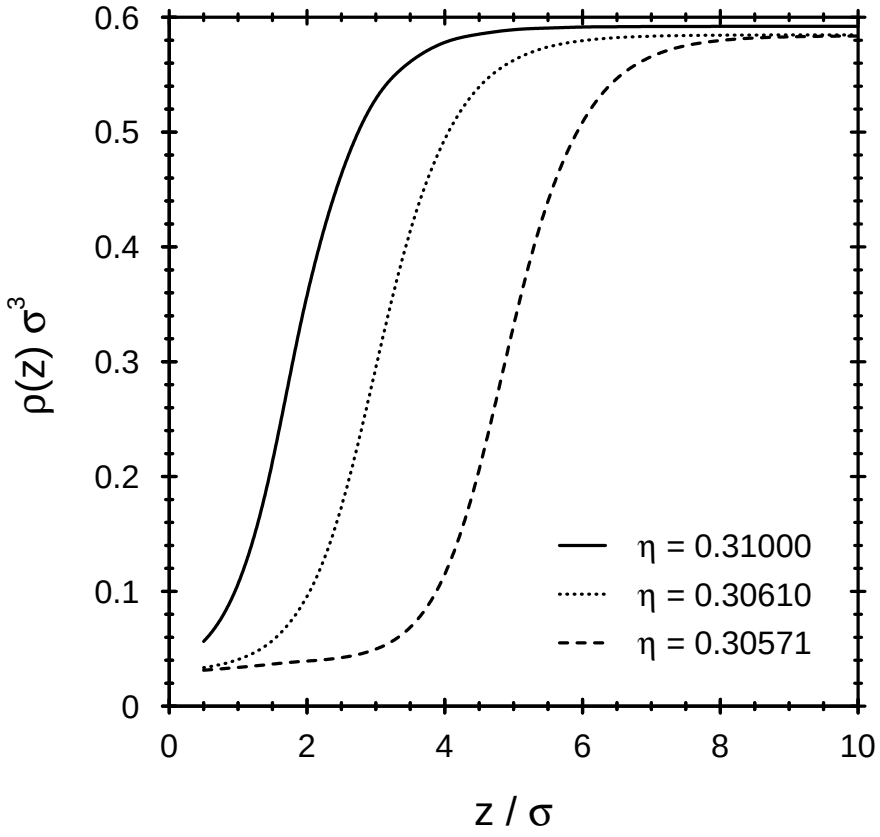

Figure 4.6: The density profiles of a square-well fluid at a planar hard wall along the path through the phase diagram shown in Fig. 4.5. $\sigma = 2R$ is the hard-sphere diameter.

with

$$\beta V_{ext}(z) = \begin{cases} \infty & z < R \\ 0 & \text{otherwise} \end{cases}$$

- minimize density functional

$$\frac{\delta\Omega[\rho]}{\delta\rho(\mathbf{r})} = 0$$

These steps are the same as for the calculation of the density profiles of the hard-sphere fluid close to the hard wall. The resulting density profiles, however, are very different. They are shown in Fig. 4.6.

Through the presence of a van der Waals loop, the pressure close to the binodal is smaller than the bulk density of the liquid, $\beta p < \rho_{bulk}$. This implies through the contact theorem mentioned above that the contact density $\rho(R^+)$ of the square-well fluid has to be smaller than the liquid bulk density. What one finds is the phenomenon called *complete drying*. The hard wall is hydrophobic and prefers the low density gas

over the high density liquid. If a liquid state point sufficiently close to bulk coexistence is considered, the square-well fluid develops a gas film close to the wall. In the drying case, the density profile of the fluid shows gas-like behavior close to the wall and a liquid behavior far away from the wall. In between one finds a vapor-liquid interface.

The thickness of the gas-like film can be measured by the excess adsorption Γ, defined by

$$\Gamma = \int dz \, (\rho(z) - \rho_{bulk}).$$

In the complete drying regime, sufficiently close to coexistence one finds

$$\Gamma \propto \ln \delta\mu,$$

with $\delta\mu = \mu - \mu_{co}$, the distance in chemical potential from its value at coexistence μ_{co}. The scenario of complete drying is completely confirmed by density functional theory.

4.3.5 Square-Well Fluid in a Slit

As a final application of density functional theory we consider the behavior of a square-well fluid in a slit geometry. The slit is made of two parallel hard walls, which are separated by a distance L. Again, to keep the application interesting we restrict the temperature to $T < T_c$ and choose the density to be in the liquid regime.

The steps to calculate the density profile in this geometry are given by

- choose liquid density ρ_{bulk} or packing fraction η, $T < T_c$
- initialize density profile

  $$\rho(z) = \rho_{bulk} \exp(-\beta V_{ext}(z))$$

  with

  $$\beta V_{ext}(z) = \begin{cases} \infty & |z| > L/2 - R \\ 0 & \text{otherwise} \end{cases}$$

- minimize density functional

  $$\frac{\delta\Omega[\rho]}{\delta\rho(\mathbf{r})} = 0$$

The state point choose for the present calculation is shown in Fig. 4.7. We choose $T/(\beta\varepsilon) = 1$ and $\eta = 0.32$. Now we keep the density of the square-well fluid fixed and vary the width of the slit L. The resulting density profiles are shown in Fig. 4.8.

We find that for large values of L a liquid in the slit. If the slit width is sufficiently small, the liquid, which is the stable bulk phase, becomes metastable compared to a gas phase. This phenomenon is called *capillary evaporation*. The reason for this

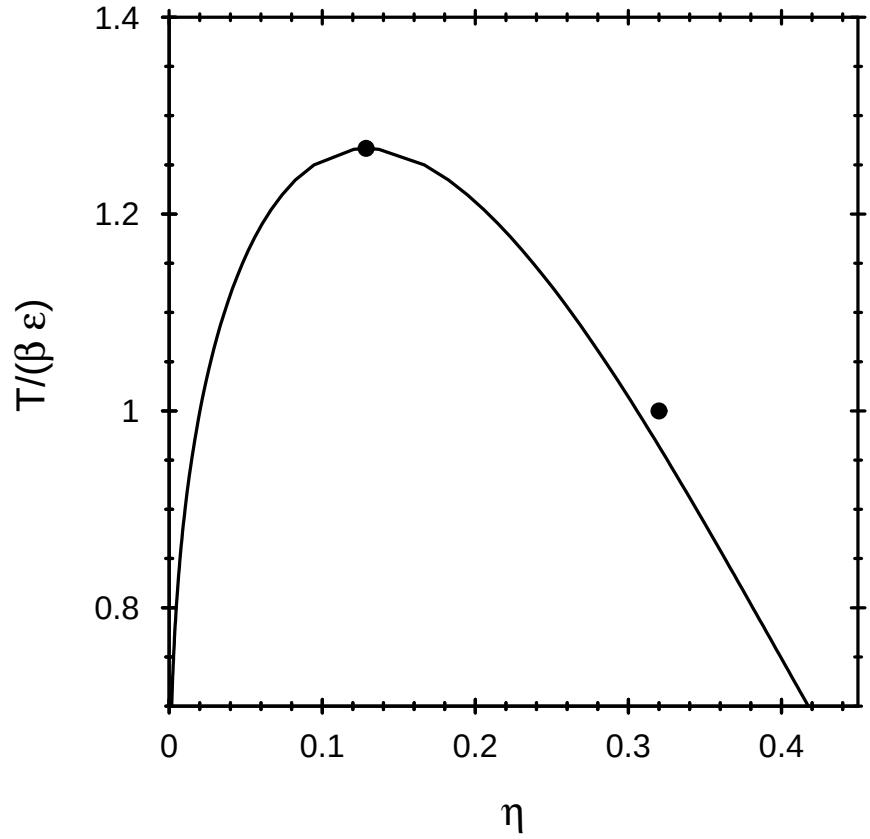

Figure 4.7: The state point of a square-well fluid in a slit geometry is indicated by the full circle.

phase transition is a competition between the volume term and the surface term in the slit geometry. To highlight this competition we recall that the grand potential Ω has the following forms:

- bulk system (unconfined):
$$\Omega = -pV$$
- fluid at a single wall:
$$\Omega_w = -pV + \gamma A$$
- fluid in a slit of width L:
$$\Omega_s \approx -pAL + 2\gamma A$$

If the wall is hydrophobic, as in the case of a hard wall, then the wall-vapor interface tension γ_v is lower than the wall-liquid interface tension γ_l. This can compete with the volume term that prefers the stable bulk phase because $p_l > p_v$.

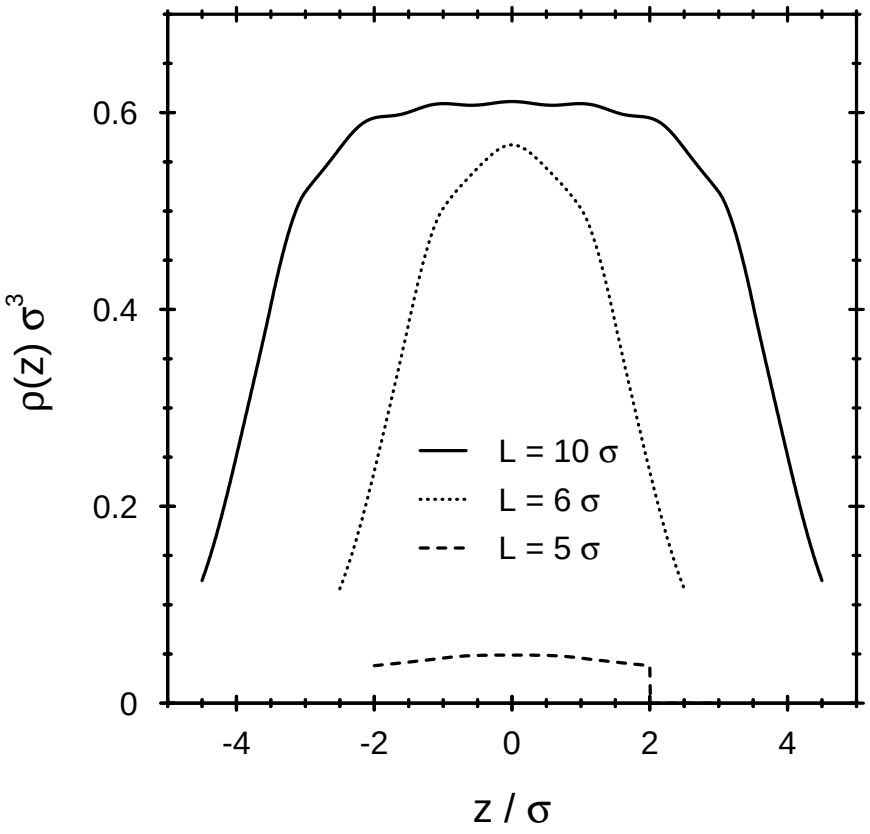

Figure 4.8: Density profiles of a square-well fluid in a slit geometry for three different values of the slit width L.

Note that in the case of a hydrophilic wall one finds $\gamma_v > \gamma_l$ and capillary evaporation cannot take place. However, a phenomenon called capillary condensation can be observed if a stable bulk vapor phase is confined in a narrow slit of hydrophilic (sufficiently attractive) walls. In that case a high density liquid, which is metastable in the bulk, is stabilized by the walls.

The main purpose of this chapter was to show that the same functional of the intrinsic excess free energy $\mathcal{F}_{ex}$ can be employed to study quite different physical scenarios simply by changing the external potential $V_{ext}(\mathbf{r})$. This is part of the power and the beauty of density functional theory.

Bibliography

[1] P. Hohenberg and W. Kohn, Phys. Rev. **136**, B 864 (1964).

[2] W. Kohn and L.J. Sham, Phys. Rev. **140**, A 1133 (1965)).

[3] N. D. Mermin, Phys. Rev. **137**, A 1441 (1965).

[4] R. Evans, Adv. Phys. **28**, 143 (1979).

[5] Evans R 1992 in *Fundamentals of Inhomogeneous Fluids* (New York: Dekker) p 85

[6] Rosenfeld Y 1989 Phys. Rev. Lett. **63** 980; see also Rosenfeld Y, Levesque D and Weis J-J 1990 J. Chem. Phys. **92** 6818

[7] Rosenfeld Y, Schmidt M, Löwen H, and Tarazona P 1996 Phys. Rev. E **55** 4245

[8] Rosenfeld Y, Schmidt M, Löwen H, and Tarazona P 1996 J. Phys.: Condens. Matter **8** L577

[9] Tarazona P and Rosenfeld Y 1997 Phys. Rev. E **55** R4873

[10] Tarazona P and Rosenfeld Y 1999 in *New Approaches to Problems in Liquid State Theory* (Dordrecht: Kluwer Academic) p 293

[11] Tarazona P 2000 Phys. Rev. Lett. **84** 694

[12] Tarazona P 2002 Physica A **306** 243

[13] See, e.g., Hansen J P and McDonald I R 1986 *Theory of Simple Liquids* (London: Academic Press)

[14] Mansoori G A, Carnahan N F, Starling K E, and Leland Jr. T W 1971 J. Chem. Phys. **54** 1523

[15] Carnahan N F and Starling K E 1969 J. Chem. Phys. **51** 635

[16] Tarazona P 1985 Phys. Rev. A **31**, 2672

[17] Gonzalez A, White J A, and Evans R 1997 J. Phys.: Condens. Matter **9** 2375

[18] Percus J K 1976 J. Stat. Phys. **15** 505

[19] Vanderlick T K, Davis H T, and Percus J K 1989 J. Chem. Phys. **91** 7136

[20] Kierlik E and Rosinberg M L 1990 Phys Rev A **42** 3382

[21] Phan S, Kierlik E, Rosinberg M L, Bildstein B, and Kahl G 1993 Phys Rev E **48** 618

[22] Rosenfeld Y 1994 Phys. Rev. E **50** R3318

[23] Rosenfeld Y 1995 Mol. Phys. **86** 637

[24] Reiss H, Frisch H L, Helfand E, and Lebowitz J L 1960 J. Chem. Phys. **32** 119

[25] González A, White J A, Román F L, Velasco S, and Evans R 1997 Phys. Rev. Lett. **79** 2466

[26] González A, White J A, Román F L, and Evans R 1998 J. Chem. Phys. **109** 3637

[27] Schmidt M, Löwen H, Brader J M, and Evans R 2000 Phys. Rev. Lett. **85** 1934

[28] Cuesta J A, Martinez-Raton Y, and Tarazona P 2002 J. Phys.: Condes. Matter **14** 11965

[29] Groot R D, van der Eerden J P, and Faber N M 1987 J. Chem. Phys. **87** 2263

[30] Groot R D, Faber N M, and van der Eerden J P 1987 Mol. Phys. **62** 861

[31] van Swol F and Henderson J R 1987 Phys. Rev. A **40** 2567

[32] Tarazona P and Evans R 1984 Mol. Phys. **52** 847

[33] Noworyta J P, Henderson D, Sokołowski D, and Chan K-Y 1998 Mol. Phys. **95** 415

[34] Roth R and Dietrich S 2000 Phys. Rev. E **62** 6926

[35] Hoover W G and Ree F H 1968 J. Chem. Phys **49** 3609

[36] Young D A and Alder J 1974 J. Chem. Phys **60** 1254

[37] Alder B J, Hoover W G, and Young D A 1968 J. Chem. Phys. **49** 3688

[38] Bryk P private communication

[39] R. Roth, R. Evans, A. Lang, and G. Kahl, J. Phys.: Condens. Matter **14**, 12063 (2002).

[40] Y.-X. Yu and J. Wu, J. Chem. Phys. **117**, 10156 (2002).

[41] H. Hansen-Goos and R. Roth, J. Chem. Phys. **124**, 154506 (2006).

[42] H. Hansen-Goos and R. Roth, J. Phys.: Condens. Matter **18**, 8413 (2006).